Lightning in global chemistry-climate models: A review of parameterizations, evaluations, and future projections

Andreas Krause[1], Francisco Javier Pérez-Invernón[2], Anja Rammig[1]

[1] Technical University of Munich, TUM School of Life Sciences, Freising, 85354, Germany
[2] Instituto de Astrofísica de Andalucía (IAA), CSIC, P.O. Box 3004, Granada, 18080, Spain
Correspondence to: Andreas Krause (andy.krause@tum.de)

Abstract. Climate models are our main tool to project how global lightning activity may change in a warmer world. However, the spatial and temporal scales involved in cloud electrification are too small to be explicitly resolved, so lightning is typically simulated using empirical relationships with proxy variables such as cloud top height (CTH), convective precipitation, the product of convective available potential energy and precipitation, or upward ice flux. This review summarizes existing global lightning parameterizations, their skill in reproducing observed lightning patterns, and their projected future changes.

We identify 19 parameterizations (including some variants) that have been applied in global modelling studies, with CTH — the earliest developed — remaining the most widely used. Most parameterizations predict total lightning, while cloud-to-ground lightning is rarely computed directly. Several parameterizations, including CTH, reproduce observed spatial lightning patterns reasonably well ($r > 0.7$), whereas precipitation-based methods perform worse (r often < 0.6). Most approaches underestimate lightning over central Africa and in mid-to-high latitudes, while overestimating activity over the Amazon and Maritime Continent. They also struggle to capture the observed land–ocean contrast in lightning activity and tend to underestimate temporal variability from diurnal to inter-annual scales.

Future projections show large uncertainty, ranging from an 11% decrease to a 44% increase in global lightning frequency per degree global warming. The mean across all parameterizations is +5.5±8.7% K^{-1} (one value per parameterization), while the mean across all individual projections (which are strongly biased towards CTH) is +7.7±8.3% K^{-1}. Although there is a broad agreement that lightning activity will increase in high latitudes, the tropical response remains highly uncertain.

1 Introduction

Lightning is an important natural source of nitrogen oxides (NO_X) in the middle and upper troposphere, an important precursor of ozone (O_3) and the hydroxyl radical (OH), thereby reducing the lifetime of methane (CH_4), and exerting strong influences on atmospheric chemistry, with implications for climate (Schumann and Huntrieser, 2007; Pickering *et al.*, 2026). Recent studies, including aircraft observations (Brune *et al.*, 2021) and laboratory experiments (Jenkins *et al.*, 2021), have revealed substantial production of lightning-generated OH. This production of OH may have a major impact on tropospheric chemistry, significantly influencing the levels of tropospheric carbon monoxide (CO), O_3, and reactive nitrogen (Mao *et al.*, 2021). On ground, lightning poses hazards to infrastructure, people, and animals (Yair, 2018). Lightning also affects vegetation, either directly when lightning strikes a tree (Krause *et al.*, 2025; Yanoviak *et al.*, 2020) or indirectly by igniting wildfires (Krause *et*

al., 2014; Felsberg *et al.*, 2018). It is thus crucial to adequately represent lightning in global atmospheric models to reliably project changes in lightning activity in a warmer climate and associated impacts on nature and society.

Although the precise mechanism responsible for lightning initiation remains an open question (e.g., Pasko *et al.*, 2025), it is well established that lightning requires strong electric fields generated by charge separation within clouds (Lopez, 2016; Saunders, 1993). The dominant explanation for charge separation is the non-inductive mechanism, in which charge separation results from collisions between small ice particles or snowflakes (grown by vapour diffusion) and larger graupel particles (formed by accretion of supercooled water droplets) in the mixed-phase region (between the 0°C and –40 °C isotherms) of the cloud (Takahashi, 1978; Price, 2013). These conditions are typically found in the presence of strong updrafts in storms, i.e. areas with strong convective activity, which carry the hydrometeors into the mixed-phase region and enhance the collisions between particles. Once charges are exchanged, lighter, positively charged ice particles are carried upward by convection, while heavier, negatively charged graupel pellets maintain lower in the cloud. This results in a dipole structure in thunderstorm clouds, with positive charges in the upper part of the cloud and negative charge below. At temperatures above –10 °C, the polarity of charge transfer is often reversed, leading to a thin positive layer near the cloud base. Lightning occurs once the electric field surpasses a critical threshold.

Recent estimates suggest that almost 60 lightning flashes occur worldwide every second (Cecil *et al.*, 2026b) — significantly higher than previously believed (Cecil *et al.*, 2014), largely due to updated estimates of the sensors' detection efficiency. Around 20-25% of all flashes reach the ground, while the remainder occur within or between clouds (Mackerras *et al.*, 1998; Whaley *et al.*, 2024). Earlier studies assumed that the cloud-to-ground (CG) fraction generally increases with latitude (Price and Rind, 1993; Prentice and Mackerras, 1977; Bandholnopparat *et al.*, 2020), but combining up-to-date datasets of total and CG lightning indicates this may actually not be the case, at least within the tropics and subtropics (Fig. 1). The spatial-temporal variability of lightning is driven by climatic conditions. Most lightning occurs over tropical land areas, where intense solar heating drives deep convection (Fig. 1). Among these regions, Central Africa experiences the highest lightning activity, followed by South America and Southeast Asia, whereas the ranking is reversed for precipitation (Price, 2013; Williams, 2005). At finer spatial scale, the highest mean flash densities are over Lake Maracaibo in Venezuela, while regions such as Cuba and northern Pakistan also reach comparable peak values (Cecil *et al.*, 2026b). Interestingly, lightning is rare over the very rainy maritime regions along the Intertropical Convergence Zone. Different mechanisms have been proposed to be responsible for the land–ocean contrast in lightning activity, including the aerosol hypothesis (more aerosols over land result in more numerous, smaller cloud droplets and potentially more intense convection) and the thermal hypothesis (the land warms faster, enhancing convection) (Williams and Stanfill, 2002; Qie *et al.*, 2024; Abbott *et al.*, 2025), but the issue is still debated and might be explained by a combination of several factors.

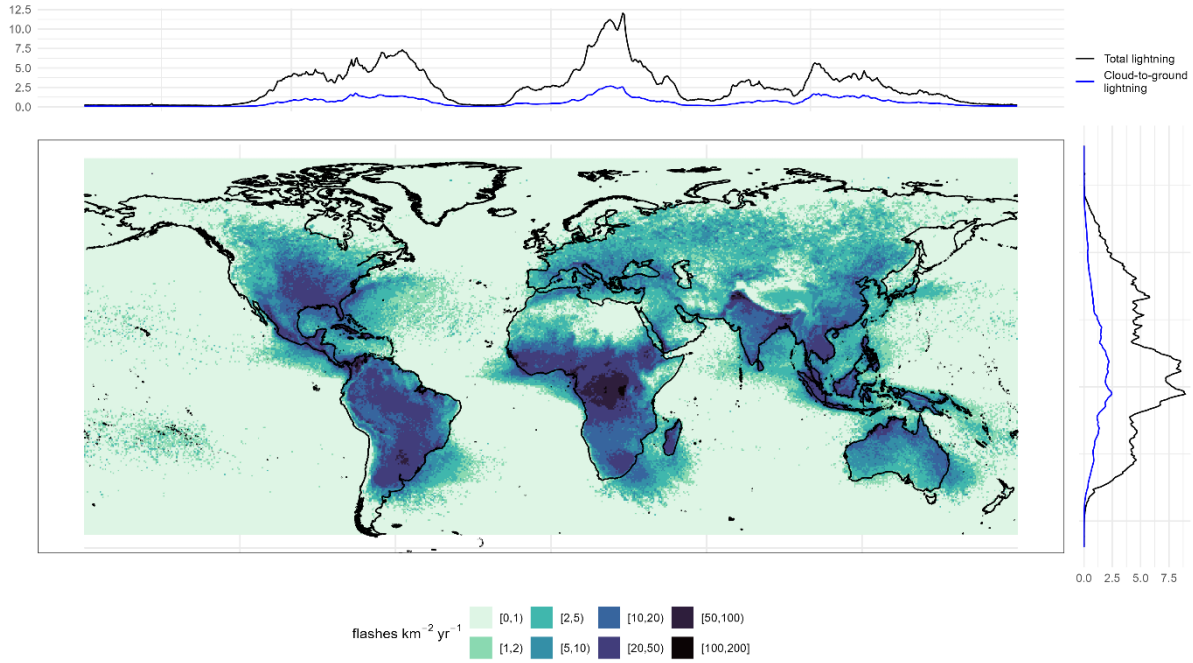


Figure 1: Global distribution of total lightning (1995-2023) according to the satellite-based combined climatology from Optical Transient Detector (OTD) and Lightning Imaging Sensor (LIS) (Cecil, 2025). The longitudinal and latitudinal mean lightning densities [flashes km^{-2} yr^{-1}] are shown on the top and right of the map. Black lines display total lightning according to LIS/OTD, while blue lines display CG lightning according to the ground-based Flash Location Aggregation from Strokes into a High-resolution Multi-scale Analysis Product (FLASHMAP, 2019-2025) (Qu *et al.*, 2026). LIS/OTD and FLASHMAP are used here because they provide well-characterized, gridded global observations that are particularly suitable for comparison with global model output. LIS/OTD provides a near-global benchmark of total lightning independent of ground-based network coverage, while FLASHMAP provides a more recent, high-resolution product of CG lightning.

On short time scales, there is a clear relationship between temperature fluctuations and lightning activity (Williams, 2005). For example, lightning activity over land is higher during hot afternoons than during the cooler night and higher during summer than during winter (Schumann and Huntrieser, 2007). The inter-annual variability of lightning also shows a strong correlation with El Niño variability (Murray *et al.*, 2012), consistent with the sensitivity of lightning to large-scale temperature fluctuations (Williams, 1992). Observations of Schumann resonance intensity further indicate substantial day-to-day variability in global lightning activity associated with large-scale land-surface temperature anomalies during cold-air outbreaks (Bozóki *et al.*, 2023). Using space-borne lightning observations and reanalysis data, Reeve and Toumi (1999) estimated a 40±14% increase in lightning activity per degree increase in average land wet-bulb temperature, a measure that incorporates both air temperature and humidity. A follow-up study found a lightning sensitivity of 17±7% per degree increase in seasonal surface air temperature (Ma *et al.*, 2005). However, whether the observed relationship between temperature and lightning also holds on even longer time scales, such as decades to centuries, remains uncertain. This is largely due to the limited availability of reliable long-term lightning observations, which hinders our ability to fully assess how lightning responds to climate change. High-quality

satellite observations only cover a period of around 25 years and do not reveal a clear trend in (sub)tropical lightning activity (Blakeslee *et al.*, 2020; Cecil *et al.*, 2026b; Pickering *et al.*, 2026). In contrast, thunderstorm day counts, which extend further back, suggest increasing activity in many lightning hotspots over the past four decades. However, they are only an indirect proxy, and regional trends in thunderstorm days and lightning frequency during the overlapping period do not always align (Lavigne *et al.*, 2019). Holzworth *et al.* (2021) reported an enhancement in the fraction of lightning strokes detected by the ground-based World Wide Lightning Location Network (WWLLN) occurring above 65°N between 2010 and 2020, coinciding with a concurrent increase in temperature. Nevertheless, additional years of data are required to robustly assess potential temperature correlations and to disentangle the possible influence of the solar cycle. Given these observational constraints, estimates of how lightning responds to historical — and especially future — climate change rely primarily on climate model simulations.

In this review, we examine existing approaches for representing lightning in global chemistry-climate models, evaluate their ability to reproduce present-day lightning patterns, and discuss their projections under a warmer climate. Relevant studies were identified through a Web of Science search using the term "lightning AND (parameterization OR parameterisation OR parametrization OR parametrisation) AND model" and by examining references cited in the retrieved papers as well as by our own knowledge of the scientific literature.

2 Lightning parameterizations in global chemistry-climate models

Global climate models, Earth System Models, and chemical transport models are our main tools for estimating future changes in global lightning activity. While lightning itself does not require atmospheric chemistry to be simulated, lightning is often included in chemical transport models because of its impacts on atmospheric composition and chemistry. However, the microphysical processes that drive cloud electrification involve temporal and spatial scales that are too fine to be explicitly resolved even by state-of-the-art global chemistry-climate models due to computational constraints (Murray, 2018). Consequently, lightning cannot be simulated directly and must instead be represented through so-called parameterizations — empirical or theoretical relationships that link lightning activity to larger-scale proxy variables available from the model. These parameterizations generally aim to predict either the lightning flash rate (F, flashes per unit time per model or satellite grid-cell), the flash density (f, flashes per unit time and area), or lightning occurrence (a probability that can be binarized using a threshold). In many model configurations, global scaling factors have to be applied to reproduce the global lightning frequency observed from space (Tost *et al.*, 2007; Finney *et al.*, 2014; Gordillo-Vázquez *et al.*, 2019). In chemical transport models it is also common to apply additional scaling factors to improve simulations of lightning-produced NO_X (Murray *et al.*, 2012; Pérez-Invernón *et al.*, 2025).

Lightning is ultimately associated with charge separation in convective clouds. Although the detailed microphysical mechanisms remain incompletely understood, non-inductive charging through collisions among ice-phase hydrometeors in the mixed-phase region is widely considered a key mechanism. The intensity of lightning therefore depends on several aspects of

convection, including atmospheric instability, the depth and strength of updrafts, and the availability and transport of ice-phase hydrometeors. Different parameterizations approximate different parts of this chain. Consequently, any variable that scales with the strength, depth, or ice/graupel loading of convective updrafts is, in principle, a viable proxy for lightning — the parameterizations reviewed below differ mainly in how directly they represent this chain of causation, and in what information is realistically available from a given model's convection and microphysics schemes.

2.1 Cloud-depth-based parameterizations

The first global lightning parameterization used convective cloud top height (**CTH**) as a proxy for lightning flash rate (Price and Rind, 1992). In terms of the processes outlined above, CTH represents lightning only indirectly: deeper convective clouds tend to be associated with stronger convection and a greater vertical extent over which electrification can occur, but CTH does not explicitly describe updraft intensity or mixed-phase microphysics. Its use as a lightning predictor was motivated by both theoretical scaling arguments and observations showing a strong relationship between storm height and lightning activity. The theoretical basis originates from Vonnegut (1963) and was subsequently further developed by Williams (1985). In this framework, a thunderstorm is conceptualized as an electric dipole with two equal but opposite charge volumes. Assuming approximately constant charge density and geometrical similarity of thunderstorms, the characteristic electric field scales with storm size L, which is assumed to be proportional to CTH, while the potential difference scales as L^2. The charging current I scales with the product of charge transport velocity V and cloud cross-sectional area ($I \propto VL^2$), such that electrical power P scales as $P \propto VL^4$. Assuming further that charge transport velocity scales with convective velocity, that convective velocity increases approximately linearly with storm height ($V \propto L$), and that lightning flash rate is proportional to electrical power gives the fifth-power relationship $F \propto L^5$. Williams (1985) found this scaling to be consistent with observations from New England, Florida, and New Mexico, which yielded exponents of 5.0, 4.7, and 4.9, respectively.

Price and Rind translated this relationship into a parameterization suitable for global models, using CTHs from the International Satellite Cloud Climatology Project (ISCCP) to estimate global lightning distribution. They evaluated the resulting distribution against global lightning observations from the Defense Meteorological Satellite Program and regional sferics observations from Southern Africa. Because no comparable direct observations of flash rate as a function of CTH were available for maritime thunderstorms, Price and Rind (1992) derived the ocean relationship indirectly. They related maximum updraft velocity to CTH separately for continental and maritime clouds and assumed that the relationship between updraft velocity and flash rate derived over land was also applicable over the ocean. This yielded a separate relationship for ocean grid boxes:

$$F_L = 3.44 \times 10^{-5}\ CTH^{4.9} \quad (1)$$

$$F_O = 6.40 \times 10^{-4}\ CTH^{1.73} \quad (2)$$

where F_L and F_O denote lightning flash rate per land or ocean grid-cell [flashes min^{-1}] and CTH is expressed in km above ground. Thus, rather than requiring CTH itself to explain the land–ocean contrast, the parameterization incorporates this contrast empirically through separate relationships. Price and Rind (1992) also proposed an alternative formulation based on peak updraft velocity, which is more directly related to convective intensity but is not universally available from model

convection schemes. CTH therefore offered the practical advantage of being readily available from both satellite observations and global models.

However, the ocean parameterization (Eq. 2) suffered from a scarcity of maritime lightning observations at the time of its derivation and later turned out to substantially underestimate lightning over the oceans. Boccippio (2002) subsequently showed that the derivation contained a formal inconsistency in the underlying scaling relationships and could produce nonphysical behaviour when the relationships were inverted. Boccippio (2002) therefore re-examined the scaling framework and formulated self-consistent relationships between flash rate, updraft velocity, and storm height based on the original Vonnegut framework. Combining the generator-power scaling with empirical relationships between updraft velocity and CTH resulted in substantially more similar CTH exponents over land and ocean than in Price and Rind (1992), 5.09 and 4.38, respectively, compared with 4.9 and 1.73. Boccippio (2002) also considered an alternative framework in which flash rate scales with generator current rather than electrical power, implying a weaker dependence on storm geometry and a stronger dependence on the rate of charge generation. More recently, Luhar *et al.* (2021) revisited these relationships and derived updated parameterizations following Boccippio's framework. When implemented in the ACCESS-UKCA chemistry–climate model, the revised oceanic parameterization substantially improved the representation of oceanic lightning compared with the original CTH parameterization. Thus, the strongly different exponents in the original CTH land and ocean relationships can be interpreted primarily as a consequence of the empirical assumptions used to derive the original ocean relationship rather than evidence for fundamentally different physical scaling laws over land and ocean.

A further difficulty arises when relationships derived for individual thunderstorms are applied at the scale of climate model grid-cells. Price and Rind (1994b) noted that diagnosed CTH depends on horizontal resolution because deep convective cores occupy only a fraction of a grid-cell. When convective fields are spatially averaged over increasingly larger areas, the maximum CTH is progressively smoothed, reducing the representation of localized deep convection. Because flash rate depends nonlinearly on CTH, calculating lightning from this spatially averaged CTH can yield substantially lower flash rates than calculating lightning separately from the underlying fine-scale convective structures. Price and Rind (1994b) therefore derived an empirical resolution-dependent correction to the CTH-based flash rate, based on the decrease in maximum CTH when convective fields were averaged over progressively larger spatial areas. This correction compensates for the loss of resolved convective extremes at coarse resolution and reduces the resulting dependence of simulated lightning on model grid size. More recently, Stolz *et al.* (2021) addressed a related but distinct scale mismatch in applying the CTH parameterization to coarse-resolution models. The original Price and Rind (1992) relationships predict flash rate per thunderstorm, whereas global models require a flash density representative of the entire grid-cell. While the spatial correction of Price and Rind (1994b) accounts for the smoothing of CTH resulting from spatial averaging, it does not explicitly account for the number of thunderstorms within a grid-cell. Stolz *et al.* (2021) therefore estimated the number of thunderstorm complexes from the modelled convective area and an assumed characteristic storm area (1,000 km² over land and 10,000 km² over ocean). They then multiplied the CTH-derived flash rate per storm by the estimated number of storms and normalized by grid-cell area to obtain grid-cell flash density.

The CTH framework was subsequently extended to partition total lightning into cloud-to-ground (CG) and intracloud (IC) flashes. Price and Rind (1993) argued that the IC/CG ratio is more closely related to the vertical extent of the cold part of a thunderstorm than to the absolute height of the freezing level. This was motivated by the occurrence of charge separation in the mixed-phase region above the freezing level: as the cold-cloud region becomes deeper, its volume and the separation between charge centers can increase, favouring IC discharges. They therefore related the ratio z=IC/CG to cold-cloud depth (CCD), defined as the vertical distance between the 0 °C level and cloud top. The relationship was derived from 139 thunderstorms over the western United States during summer 1988, combining radar-derived CTH, radiosonde-derived freezing-level heights, and observed CG lightning. Because IC and total lightning were not directly observed, total lightning was estimated using Eq. 1, and IC lightning was subsequently inferred as the difference between parameterized total and observed CG lightning. The resulting semi-empirical relationship was:

$$z = 63.09 - 36.54 \cdot CCD + 7.493 \cdot CCD^2 - 0.648 \cdot CCD^3 + 0.021 \cdot CCD^4 \quad (3)$$

where CCD is in km and the relationship is valid for $5.5<CCD<14$ km.

Some studies retained the CTH proxy but updated the relationship to account for additional processes. For instance, Michalon *et al.* (1999) argued that differences in cloud droplet concentrations (CDC) could contribute to the contrast between continental and maritime lightning activity (**CTH-CDC**). Based on dimensional scaling arguments, they proposed a dependence of lightning frequency on $CDC^{2/3}$ while retaining an approximately fifth-power dependence on CTH. Because CDC was not simulated explicitly, representative values were assumed for continental (600 mg^{-1}) and maritime (50 mg^{-1}) conditions. The resulting ocean relationship is:

$$F_O = 6.57 \times 10^{-6}\ CTH^{4.9} \quad (4)$$

This retained the same CTH exponent as over land while representing part of the land–ocean difference through prescribed cloud microphysical conditions.

Grewe *et al.* (2001) similarly retained a geometrical measure of storm size but replaced absolute CTH with cloud thickness and incorporated information on convective intensity. Their parameterization combines cloud thickness with an indicator of the updraft strength (**US**) derived from the parameterized convective upward mass flux:

$$F = 1.54 \times 10^{-5}\ (wd^{0.5})^{4.9} \quad (5)$$

where w is an indicator of updraft strength [m s^{-1}] and d the cloud thickness [m]. The relationship was derived to reproduce the continental CTH-based flash rates of Price and Rind (1992), rather than being independently calibrated against lightning observations. The approach therefore modifies the original CTH parameterization by combining cloud size with information on convective intensity, while assuming that differences in convection intensity between land and ocean are captured by the model, so no separate equations are required.

Yoshida *et al.* (2009) further refined the geometrical measure by modifying how cloud depth is defined. They argued that the full cloud depth is not necessarily the most relevant quantity for electrification because charge separation is primarily associated with interactions among ice-phase hydrometeors in the mixed-phase region. They therefore introduced cold-cloud depth (**CCD**), defined as the vertical distance between the radar-derived storm top and the 0 °C melting level. Unlike CTH,

CCD accounts for variations in the altitude of the freezing level and more directly represents the vertical extent of the ice-containing part of the cloud. This distinction is also relevant under climate warming, as an increase in CTH accompanied by a rising freezing level does not necessarily imply a corresponding increase in the depth of the cloud region relevant for electrification. Using eight years (1998–2005) of coincident TRMM Precipitation Radar and LIS observations, Yoshida et al. related CCD to the number of lightning flashes per second per convective cloud (NFSC). They found an approximately fifth-power relationship across all three regions considered, but with substantially different prefactors:

$$NFSC_L = 1.58 \times 10^{-6}\ CCD^{4.9} \quad (6)$$

$$NFSC_o = 1.26 \times 10^{-7}\ CCD^{5.1} \quad (7)$$

$$NFSC_{MaritimeContinent} = 5.01 \times 10^{-7}\ CCD^{5.1} \quad (8)$$

where NFSC is the number of flashes per second per convective cloud and CCD is in km. The coefficients correspond to the mean logarithmic prefactors of −5.8, −6.9, and −6.3 reported for land, ocean, and the Maritime Continent, respectively. Thus, while the exponent is remarkably consistent among regions, the approximately order-of-magnitude difference in the prefactor between land and ocean indicates substantially greater lightning activity in continental clouds for a given CCD. These relationships were subsequently implemented in the global CAM5 model by Clark *et al.* (2017). The observed present-day spatial lightning distribution was captured almost as well as with the CTH parameterization (spatial correlations of 0.80 and 0.83, respectively).

Overall, cloud-depth-based parameterizations represent lightning through a readily available but relatively indirect measure of convective activity. Their simplicity has facilitated widespread application in global models, but two limitations are particularly important. First, storms with similar CTH or CCD can differ substantially in updraft strength and mixed-phase microphysics and consequently in lightning activity. Second, the strong nonlinear dependence on cloud depth amplifies biases in the simulated predictor: for a fifth-power relationship, a 10% increase in cloud depth corresponds to a 61% increase in predicted flash rate, all else being equal. These limitations motivated parameterizations based more directly on convective intensity and the transport and abundance of ice-phase hydrometeors, which are discussed in the following sections.

2.2 Convective intensity-based parameterizations

Some studies moved away from cloud geometry and instead related lightning to measures of convective intensity, convective precipitation, or the vertical transport of air. Meijer *et al.* (2001) found a simple empirical linear relationship between convective precipitation (from ECWMF meteorological fields) and the number of CG lightning flashes detected by ground-based lightning observations over central Europe during summer 1998 (**CP_Linear**):

$$F_{CG} = 14700\ CP + 1.7 \quad (9)$$

where CP is the accumulated convective precipitation [m] over a 6-hour period. Convective precipitation showed substantially better spatial agreement with lightning than CTH (average match frequency 0.81 vs. 0.30). This may have been related to the coarse temporal sampling of simulated CTH relative to the short lifetime of thunderstorms. While the authors did not provide a separate ocean equation, some global modelling studies assumed a 90% reduced flash rate over the oceans to account for the

higher rain yields per flash typically observed in maritime convection (e.g. Boersma *et al.*, 2005; Finney *et al.*, 2014). If necessary, the predicted CG lightning can be converted to total lightning e.g., using the formula of Price and Rind (1993, Eq. 3).

Allen and Pickering (2002), building upon earlier work (Allen *et al.*, 2000), proposed a fourth-order polynomial parameterization based on upward mass flux at 440 hPa (**MFLUX**), providing a more direct measure of convective vertical transport than either CTH or surface precipitation. They fitted mass flux from GEOS-STRAT meteorological fields against observed CG lightning observations over the US and nearby locations during 1997:

$$F_{CG}=\frac{\Delta x\Delta y}{A}\left(-2.34\times10^{-2}+3.08\times10^{-1}\,M-7.19\times10^{-1}\,M^2+5.23\times10^{-1}\,M^3-3.71\times10^{-2}\,M^4\right) \quad (10)$$

where F_{CG} is the flash rate [flashes min^{-1}] within the 2.0°x2.5° grid-cell, $\Delta x\Delta y$ is the cell area, A the area of a 2.0°×2.5° cell centred at 30°N (~53,500 km²), and M the upward cloud mass flux [kg m^{-2} min^{-1}] at an altitude of 0.44 sigma (~440 hPa). For $M < 0$ or $M > 9.6$, values are capped at the nearest bound. Given the low sensitivity of this fit to surface type, no distinction is usually made between land and ocean grid boxes. Allen *et al.* (2010) subsequently modified the MFLUX formulation by introducing a thresholded power-law dependence on upward cloud mass flux and scaling factors to better reproduce the observed spatial and temporal distribution of lightning.

Allen and Pickering (2002) also suggested an alternative polynomial parameterization based on convective precipitation (**CP_Poly**), which explicitly distinguishes between land and ocean:

$$F_{CG_L}=\frac{\Delta x\Delta y}{A}\left(3.75\times10^{-2}-4.76\times10^{-2}\,CP+5.41\times10^{-3}\,CP^2+3.21\times10^{-4}\,CP^3-2.93\times10^{-6}\,CP^4\right) \quad (11)$$

$$F_{CG_O}=\frac{\Delta x\Delta y}{A}\left(5.23\times10^{-2}-4.80\times10^{-2}\,CP+5.45\times10^{-3}\,CP^2+3.68\times10^{-5}\,CP^3-2.42\times10^{-7}\,CP^4\right) \quad (12)$$

where CP is the convective precipitation rate at the surface [mm day^{-1}], set to 0 for precipitation rates less than 7 mm day^{-1} and capped at 90 mm day^{-1}. As a slight modification, Magi (2015) proposed fifth-order polynomial parameterizations of convective mass flux and convective precipitation to predict total lightning.

Romps *et al.* (2014) took a different approach, finding that CG lightning over the contiguous US can be largely predicted by the product of convective available potential energy (CAPE; a measure of atmospheric instability) and precipitation rate P (**CAPE×P**). They interpreted CAPE×P as a measure of the rate at which convection supplies kinetic energy to precipitating water, and assumed that lightning dissipates a roughly constant fraction of this energy. Notably, the authors did not propose a particular charging mechanism. They calibrated their equation against CG lightning observations over the contiguous US in 2011:

$$f_{CG} = \eta/E \times CAPE \times P \quad (13)$$

where f_{CG} is the CG lightning density [flashes m^{-2} s^{-1}], η/E is the constant of proportionality with a value of 1.3×10^{-11} J^{-1}, CAPE is in J kg^{-1} and P in kg m^{-2} s^{-1}. This approach increased the explained variance in the 2011 CONUS time series from 39% for the CTH approach to 77% for CAPE×P. However, the approach later turned out to overestimate lightning over the oceans (Romps *et al.*, 2018). The authors concluded that factors other than CAPE and precipitation must contribute to the land–ocean contrast. Cheng *et al.* (2021) subsequently showed that lightning over the tropical ocean is strongly suppressed at

low CAPE and attributed this to the smaller size of oceanic storms and stronger entrainment, which limits updraft strength. They proposed and tested a modification of the CAPE×P scheme in which CAPE over the ocean is replaced by max(CAPE – 225, 0) thereby suppressing lightning entirely for CAPE below 225 J kg^{-1}. While this substantially improved the simulated land–ocean contrast, so far no global modelling study has adopted this modification.

2.3 Microphysical parameterizations

A further group of parameterizations attempts to represent lightning more directly through the microphysical processes associated with charge separation. Non-inductive charging is thought to result from collisions between ice-phase hydrometeors with different phase and microphysical properties in the mixed-phase region. Variables describing the abundance and upward transport of ice-phase hydrometeors therefore provide a more direct proxy for the charging process than cloud depth, CAPE, or precipitation alone. Finney *et al.* (2014) developed a lightning parameterization based on the ERA-Interim upward cloud ice flux (**IFLUX**) at 440 hPa, representative of the mid-tropospheric mixed-phase region where charge separation between ice crystals and graupel occurs. The parameterization was calibrated against LIS lightning observations for 2002:

$$f_L = 6.58 \times 10^{-7}\ q \times \Phi_{mass} / c \quad (14)$$

$$f_O = 9.08 \times 10^{-8}\ q \times \Phi_{mass} / c \quad (15)$$

where f is the flash density [flashes $m^{-2}\ s^{-1}$], q is the specific cloud ice water content at 440 hPa [kg ice per kg air], Φ_{mass} the updraft mass flux at 440 hPa [kg air $m^{-2}\ s^{-1}$], and c the fractional cloud cover at 440 hPa. The division by cloud fraction converts the grid-cell mean mass flux to a flux per unit cloudy area, thereby estimating the intensity of upward ice transport within clouds. The separate land and ocean coefficients further account empirically for differences in the relationship between upward ice transport and lightning over the two surfaces. When evaluated against independent LIS observations for 2007-2011, the parameterization improved the representation of the spatial distribution of lightning, with the annual spatial correlation increasing from 0.62 for CTH to 0.77 for IFLUX, while RMSE decreased from 9.10 to 4.53 flashes $km^{-2}\ yr^{-1}$.

Finney *et al.* (2018) subsequently adjusted the sampling level from 440 hPa to 390 hPa for future climate simulations, to account for the expected rise of the tropopause and associated shift in the vertical temperature profile under warming. Romps (2019) later modified this scheme further by using the upward cloud ice flux at the 260 K isotherm (**IFLUX_T**), which lies within the mixed-phase region, instead of a fixed pressure level, arguing that a temperature-based reference is more physically appropriate for climate change simulations, where the height of cloud charge separation can shift with warming.

Lopez (2016) developed another microphysics-informed parameterization for the European Centre for Medium-Range Weather Forecasts (ECMWF) model that combines convective cloud base height (CBH), CAPE, and a proxy representing the charging rate resulting from the collisions between graupel and other types of hydrometeors (Q_R) (**Q-CAPE-CBH**):

$$f = a\ Q_R\ CAPE^{0.5}\ \min(CBH, 1.8)^2 \quad (16)$$

where f is the lightning density [flashes $km^{-2}\ day^{-1}$], a is a constant obtained after calibration against the LIS/OTD lightning climatology, Q_R [kg m^{-2}] is computed from the amounts of graupel multiplied by the combined snow and liquid water content

in the charge separation region between the 0° and -25°C isotherms, CAPE is in J kg^{-1}, and CBH in km. While Finney *et al.* (2014) represented the non-inductive charging process using the upward cloud-ice flux at a single atmospheric level (440 hPa), Lopez (2016) explicitly represented the coexistence of interacting hydrometeor species throughout the mixed-phase region and combined this with proxies for convective intensity (CAPE) and updraft size (CBH). Notably, the parameterization partitions frozen precipitation into graupel and snow differently for land and ocean grid boxes, which was found necessary to reproduce the observed land–ocean contrast. However, Lopez (2016) acknowledged that this distinction was crude because suitable global observations of frozen hydrometeors were unavailable. In 1999-2008 ECMWF simulations, Q-CAPE-CBH reproduced the spatial distribution of the LIS/OTD climatology better (r=0.88) than CTH (r=0.73).

Lopez (2016) noted that Q_R bears some similarity to one of two lightning proxies developed by McCaul *et al.* (2009) from convection-resolving simulations. McCaul et al. related lightning either to the upward graupel flux at the -15 °C level, which better captured temporal variability, or to the vertically integrated amount of graupel, snow, and cloud ice in each model column, which better represented the spatial extent of lightning. While the latter sums the abundance of different ice hydrometeors, Lopez (2016) instead used the product of graupel and other hydrometeor concentrations as a proxy for their interactions and associated charge generation. He *et al.* (2022) subsequently modified the Lopez scheme to more closely follow the second approach of McCaul *et al.* (2009), replacing the collision-based Q_R proxy with the column-integrated amount of cloud ice, snow, and graupel within the 0 to −25 °C charging region (Q_{Ra}) and combining it with CAPE (**Q-CAPE**):

$$f_L = a_1 \, Q_{Ra} \, CAPE^{1.3} \quad (17)$$

$$f_O = a_2 \, Q_{Ra} \, CAPE^{1.3} \quad (18)$$

where f is the lightning density [flashes m^{-2} s^{-1}], a_1 and a_2 are constants obtained after calibration against LIS/OTD lightning observations, Q_{Ra} in kg m^{-2}, and CAPE in J kg^{-1}. Thus, compared with Q-CAPE-CBH, the modification replaces the product of interacting hydrometeors with their summed column abundance, removes the dependence on CBH, and increases the dependence on CAPE from $CAPE^{0.5}$ to $CAPE^{1.3}$. These modifications increased the global spatial correlation with LIS/OTD from r=0.79 for Q-CAPE-CBH to r=0.83 for Q-CAPE. More recently, Michibata (2024) extended this approach by coupling Q-CAPE to a two-moment microphysics scheme with prognostic graupel, allowing the mass and number concentration of graupel to evolve explicitly through processes including riming, accretion, melting, and sedimentation rather than diagnosing graupel from frozen precipitation.

2.4 Multi-predictor statistical and machine-learning parameterizations

In recent years, several lightning parameterizations have moved away from a single dominant proxy and instead combine multiple large-scale environmental variables, using statistical or machine-learning approaches. Rather than representing the charging process directly, these parameterizations relate lightning activity to combinations of environmental conditions that influence deep convection, mixed-phase microphysics, and thunderstorm electrification.

Liaskos *et al.* (2015) developed an empirical lightning parameterization by initially considering five meteorological predictors: CCD, total cloud depth, CAPE, vertically integrated convective mass flux (CMF) in the cold part of the cloud (T < 263 K),

and cubed surface temperature difference relative to 273 K. However, they found that a simpler two-predictor scheme based on CMF and surface temperature (**CMF-T**), performed comparably well. The resulting parameterization calculates lightning as:

$$f_L = 6.13 \times 10^{-7} (CMF + T) \quad (19)$$

$$f_O = 3.47 \times 10^{-8} (CMF + T) \quad (20)$$

where f is the lightning density [flashes km^{-2} s^{-1}], CMF represents normalized vertically integrated convective mass flux in the cold part of the cloud, and T represents the normalized cubed surface-temperature difference relative to 273 K, set to zero for temperatures below 273 K. The parameterization was calibrated against the smoothed daily LIS/OTD climatology and reproduced the general spatial and seasonal distribution of lightning. However, no numerical evaluation metrics were reported to quantify its predictive performance.

Stolz *et al.* (2017) introduced a logarithmic multiple linear regression model with five predictors, derived from multidimensionally binned data obtained by matching TRMM-observed convective features and LIS lightning observations from 2004–2011 with environmental conditions from ERA-Interim (**ENV**):

$$\log_{10}(f_L) = 1.037 + 0.171 \log_{10}(NCAPE) + 0.169 \log_{10}(CCN) - 0.723 \log_{10}(WCD) + 0.084 \log_{10}(SHEAR) - 0.623 \log_{10}(RH) \quad (21)$$

$$\log_{10}(f_O) = 3.413 + 0.300 \log_{10}(NCAPE) + 0.174 \log_{10}(CCN) - 1.521 \log_{10}(WCD) + 0.011 \log_{10}(SHEAR) - 0.352 \log_{10}(RH) \quad (22)$$

where f is the lightning density [flashes km^{-2} min^{-1}], NCAPE is normalised CAPE [J kg^{-1} m^{-1}], CCN the aerosol number concentration N_{40} [cm^{-3}] from the GEOS-Chem-TOMAS model, used as a proxy for cloud condensation nuclei, WCD the warm cloud depth [m], SHEAR the 1000–500 hPa vertical wind shear [m s^{-1}], and RH the mean relative humidity [%] between 850 and 500 hPa. The predictors represent different environmental factors potentially influencing lightning: NCAPE characterizes atmospheric instability, CCN can affect supercooled liquid water and graupel formation through aerosol–cloud interactions, WCD influences the amount of liquid water reaching the mixed-phase region, while SHEAR and RH characterize the dynamical organization and moisture environment of convection.

A similar approach was followed by Etten-Bohm *et al.* (2021), who used logistic regression to predict lightning occurrence rather than flash density. The model relates the probability of lightning to up to seven large-scale variables from MERRA-2 reanalysis — CAPE, NCAPE, lifting condensation level (LCL), column saturation fraction, 700-hPa vertical velocity, low-level wind shear, and deep-level wind shear. Their most complex model combined these environmental predictors with geographic indicators (coast, terrain slope, and latitude) and a subset of interaction terms. However, the authors also developed two models using only the three most important predictors — CAPE, LCL, and column saturation fraction — with one of the models additionally accounting for their interactions (**ENV_Int**). The models were trained using matched LIS and MERRA-2 data from 2003 and independently tested on 2004, achieving a probability of detection for lightning occurrence of up to 86% for the most complex model. However, the simpler model using only CAPE, LCL, and column saturation fraction and their interactions performed almost as well, and was therefore suggested as a potentially more suitable parameterization for

implementation in global climate models. Notably, even the simpler model captured the observed land–ocean contrast relatively well despite not explicitly distinguishing between land and ocean, likely because the environmental predictors and their interactions differ systematically between continental and oceanic convection.

Verjans and Franzke (2025) developed a data-driven lightning parameterization combining decision trees with Extreme Learning Machines, which serve as regression models within the terminal nodes of the trees (**ELM-tree**). The model was trained on daily lightning observations spanning 1995–2023, combining OTD and LIS-TRMM data with newly processed LIS-ISS observations, together with corresponding ERA5 climate data. Nine atmospheric and geographic variables were selected from an initial set of 25 potential predictors. The approach splits the input space of climatic conditions into seven separate regimes, within which lightning densities are simulated with specific single hidden layer neural networks. Notably, surface elevation is used for the second split, with a threshold close to sea level that largely separates continental and oceanic regimes. Thus, rather than prescribing separate land and ocean equations as in several earlier parameterizations, a land–ocean distinction can emerge from the data-driven tree construction. When evaluated over six test years, the model substantially outperformed CTH and IFLUX, achieving a daily grid-cell R^2 of 0.72, compared with 0.50 for CTH and 0.49 for IFLUX.

Yin *et al.* (2026) developed a deep-learning lightning scheme based on a convolutional architecture (**ResUNet**). CAPE is the model's sole predictor variable but is provided as a two-dimensional spatial field, such that the predicted lightning at a given grid-cell can depend on CAPE both locally and in other grid-cells. This contrasts with conventional grid-cell-based parameterizations, in which lightning at each grid-cell is calculated solely from predictor values within that grid-cell. CAPE was selected following an ablation analysis of six candidate predictors derived from existing lightning parameterizations. The model was trained and evaluated against the same LIS/OTD lightning record used and extended by Verjans and Franzke (2025). Compared with ELM-tree, ResUNet increased R^2 from 0.72 to 0.89, while reducing RMSE by 38% and absolute bias by 41%. The authors interpreted the improved performance, particularly for extreme lightning, as reflecting the model's ability to capture the movement of convective systems between neighbouring grid-cells and the spatial extent of large convective systems.

Finally, Krause *et al.* (accepted) developed an XGBoost machine-learning model (**ENV_XGB**) and a multiple linear regression model (**ENV_Linear**) to predict CG lightning density over land. Both models use six near-surface atmospheric variables as predictors: air temperature, precipitation, relative humidity, pressure, wind speed, and shortwave radiation. Although these variables do not directly represent the atmospheric processes responsible for lightning generation, they were selected because they are widely available in long-term climate forcing datasets and climate model projections, including those provided by the Inter-Sectoral Impact Model Intercomparison Project (ISIMIP). This choice aimed to balance physical relevance with applicability across different climate modelling frameworks. The models were developed and cross-validated using daily CG lightning observations from FLASHMAP for 2019 and additionally evaluated against independent lightning observations from the Earth Networks Total Lightning Network (ENTLN) for 2015–2018. ENV_XGB outperformed ENV_Linear and the established CP_Linear, CP_Poly, and CAPE×P parameterizations in reproducing the spatial distribution and seasonal variability of CG lightning.

420

2.5 Synthesis

The evolution of lightning parameterizations reflects a broad progression from empirical proxies of convective development toward either more explicit representations of the processes controlling electrification or statistical approaches combining multiple environmental controls. CTH-based approaches use cloud depth as a readily available indicator of convective
425 intensity; convective precipitation-, mass-flux-, and CAPE-based schemes describe the strength or amount of convection; environmental and machine-learning approaches combine multiple controls; and microphysics-based schemes attempt to represent the ice-phase processes associated with charge separation more directly.

Presently, the CTH approach is still the most popular lightning parameterization (Fig. 2), maybe because CTH is a common variable in climate models and the parameterization is relatively robust across different models and convection schemes (Tost
430 *et al.*, 2007). For instance, it was applied in 10 out of 12 models participating in the Atmospheric Chemistry and Climate Model Intercomparison Project (Finney *et al.*, 2016b) and in all Earth System Models participating in CMIP6 (Thornhill *et al.*, 2021). In recent years, the study by Romps *et al.* (2014) has also received a lot of attention (Fig. 2a), even though the CAPE×P approach proposed by the authors has seen more limited uptake in actual modelling studies (Fig. 2b, Table S1). In fact, 69% of all identified modelling studies after 2014 included the CTH parameterization, while only 20% used CAPE×P and 12%
435 IFLUX (some studies applied multiple parameterizations).

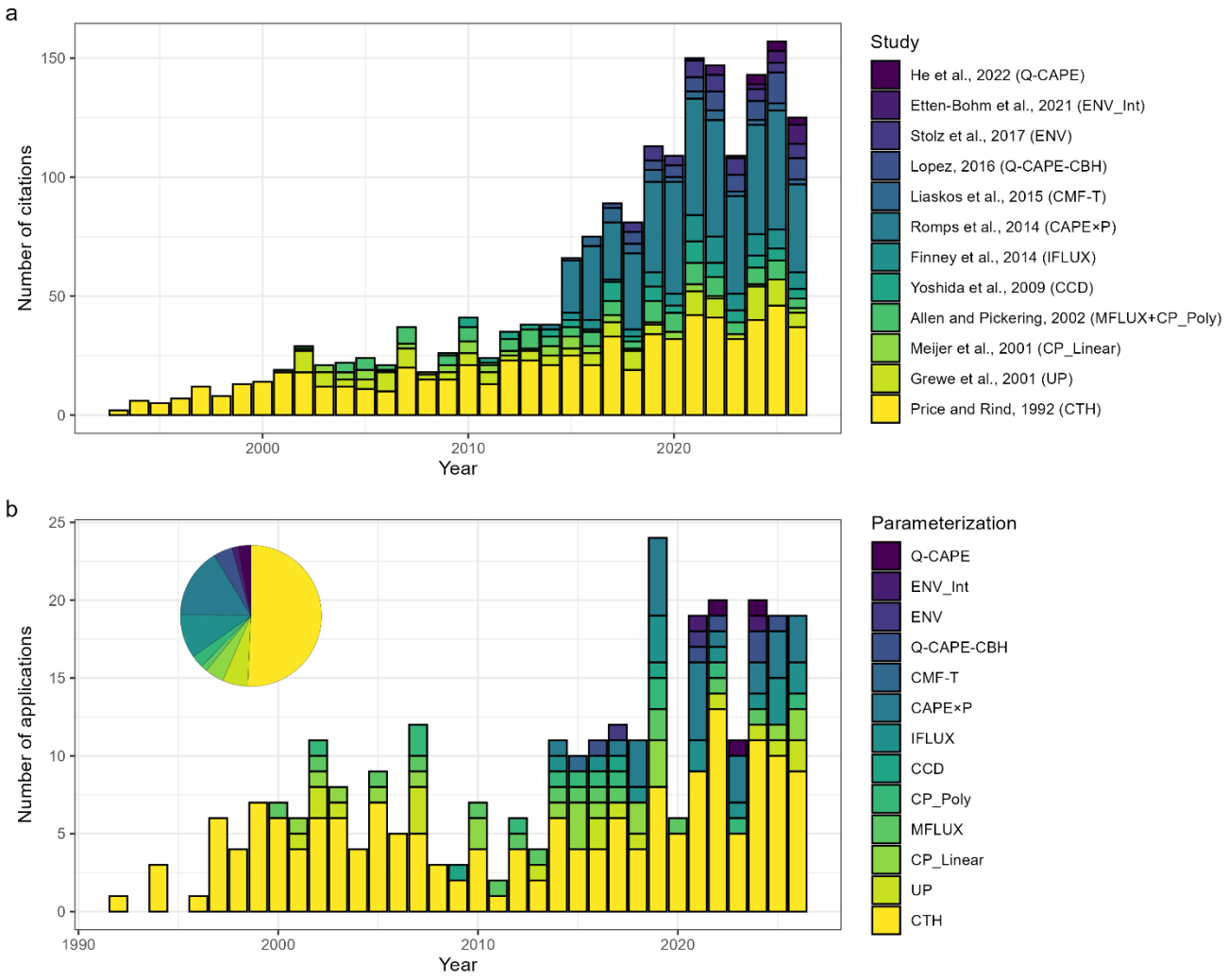


Figure 2: Popularity of different lightning parameterizations. Number of citations per year for the main reference of the parameterizations according to Web of Science (a) and number of applications of the parameterizations in actual modelling studies (b). Only parameterizations developed before 2023 are shown to enhance clarity. The pie chart indicates the fractional share of different parameterizations since 2023.

It should be noted that numerous additional lightning parameterizations exist in numerical models, many of which more directly represent the microphysical processes of cloud electrification. These are typically applied in high-resolution, cloud-resolving models that explicitly represent convection (McCaul *et al.*, 2009; Yair *et al.*, 2010; Cummings *et al.*, 2024; Fierro *et al.*, 2013). However, while computational power has increased significantly in recent years and large-scale models are beginning to explicitly represent storm-scale convective circulations (Uribe *et al.*, 2026), running these models is still

computationally expensive, especially for global, long-term climate simulations (Field *et al.*, 2018). An alternative is so-called superparameterization, in which a two-dimensional cloud-resolving model is embedded within each grid column of a conventional climate model (Charn and Parishani, 2021). Nevertheless, summarizing all existing lightning parameterizations is beyond the scope of this review. Instead, we focus here on schemes that have been applied and evaluated in global-scale modelling studies using models that do not explicitly resolve convection.

3 Evaluation of parameterizations

3.1 Lightning datasets

Lightning observations used to evaluate model parameterizations can broadly be divided into ground-based and space-based measurements. Ground-based Lightning Location Systems (LLSs) detect electromagnetic signals emitted by lightning discharges, typically in the Very Low Frequency (VLF) and Low Frequency (LF) ranges, and use Time of Arrival (TOA) methods to locate individual lightning events (Nag *et al.*, 2015). They provide continuous temporal sampling and, depending on the network, regional to global coverage. However, their detection efficiency (DE) is generally spatially heterogeneous and substantially higher for CG lightning than for IC lightning. DE can also change over time as sensor networks expand, sensors are upgraded, and processing algorithms are updated, potentially introducing artificial trends into long-term lightning records. Such changes therefore need to be considered when using LLS observations to evaluate simulated lightning densities.

The World Wide Lightning Location Network (WWLLN) is a global network of relatively sparse VLF radio sensors that detects lightning strokes, with a particular sensitivity to strong CG strokes (Kaplan and Lau, 2022, 2021). In contrast to most gridded lightning products, it is explicitly based on detected strokes rather than flashes. Its DE is relatively low and spatially heterogeneous, but comparisons with LIS/OTD indicate substantially higher detection efficiency over ocean than over land. Although DE corrections can improve the representation of the global spatial distribution, they do not eliminate all uncertainties associated with the underlying observations. The spatial patterns of WWLLN differ substantially from those of other lightning products discussed below, particularly over central Africa, where the pronounced lightning maximum observed by LIS/OTD is considerably less prominent in WWLLN. The latest version of WWLLN provides DE-corrected global stroke densities for 2010-2025 at spatial resolutions of 0.5° and 5 arc-minutes and daily and monthly temporal resolutions (Kaplan, 2026).

The Earth Networks Total Lightning Network (ENTLN) is a denser wideband sensor network operated by Earth Networks that detects and classifies both CG and IC lightning (Zhu *et al.*, 2022). Its detection performance is generally high in regions with dense sensor coverage but varies spatially. The dataset provides the location and timing of detected flashes, together with information on lightning type (CG or IC), peak current, duration, and flash multiplicity, for the 2012-2024 period. The data are available upon request for scientific applications but need to be aggregated to gridded lightning densities for comparison with global model output.

The Flash Location Aggregation from Strokes into a High-resolution Multi-scale Analysis Product (FLASHMAP) is a recently developed, freely available gridded lightning product based on spatially merged observations from Vaisala's Global Lightning Detection Network (GLD360) and the U.S. National Lightning Detection Network (NLDN) (Qu *et al.*, 2026). It provides aggregated information on both CG and IC lightning, including flash counts and multiplicity statistics, as well as stroke counts and peak-current statistics. Around 52% of the recorded flashes are classified as CG, indicating a substantial underestimation of IC flashes. FLASHMAP was validated globally against WWLLN and regionally against lightning detection networks in Australia, Spain, and Alaska. While FLASHMAP detects a lot more strokes than WWLLN over land and most ocean regions, WWLLN has higher stroke densities in some oceanic regions The spatial patterns of FLASHMAP CG lightning are broadly consistent with those observed in LIS/OTD total lightning and ENTLN CG lightning datasets (Krause *et al.*, accepted). The product is available at 0.25° daily and 0.5° monthly resolution for 2019-2025 (Qu *et al.*, 2026).

Schumann resonance (SR) measurements provide an alternative approach for monitoring global lightning activity. Lightning discharges emit extremely low-frequency electromagnetic waves that resonate in the cavity between the Earth's surface and the ionosphere and can be detected continuously from ground-based stations (Price, 2016). SR observations have therefore been used to investigate diurnal, seasonal, and inter-annual variations in global lightning activity. However, they do not directly locate individual flashes and are most suitable for evaluating large-scale or globally integrated temporal variability rather than detailed spatial patterns.

Space-based optical instruments detect short-duration emissions from the neutral oxygen triplet near 777 nm produced by lightning, observed as changes in pixel brightness from above (Blakeslee *et al.*, 2020; Cecil *et al.*, 2026b). These optical signals are then clustered into groups and flashes using spatiotemporal criteria. Because the 777-nm emission is produced by both CG and IC lightning, these instruments observe total lightning activity without directly discriminating between the two flash types. The DE of space-based optical instruments is generally high for both CG and IC lightning, but depends on factors such as time of the day, cloud thickness, discharge altitude, and field of view (Blakeslee *et al.*, 2020; Cecil *et al.*, 2026a; Murphy and Said, 2020). Space-based observations are obtained from Low Earth Orbit (LEO) or geostationary (GEO) satellites.

The most widely used LEO sensors for global lightning observations are the Optical Transient Detector (OTD) on board of the Orbview-1 satellite and the Lightning Imaging Sensor (LIS) on the Tropical Rainfall Measurement Mission (TRMM). OTD provided near-global coverage but was only operational from 04/1995 to 03/2000. In contrast, LIS only covered regions between ±38° but was active for a longer period (12/1997-04/2015). LIS also achieved a higher DE, recently estimated at 59-71%, compared to 22-52% for OTD (Cecil *et al.*, 2026a). Data from both sensors are included in the joint LIS/OTD products, which are consequently more robust in the tropics. More recently, the "successor" of TRMM-LIS, ISS-LIS, operated on board the International Space Station (ISS) from 03/2017 to 11/2023 and extended observations to approximately 55°S–55°N (Cecil *et al.*, 2026a). LIS/OTD are among the most extensively characterized global lightning observations, with their detection performance evaluated through coincident comparisons with ground-based lightning networks and other independent observations, as well as dedicated instrument and algorithm validation. The LIS/OTD products have been widely used to develop and evaluate lightning parameterizations because they provide near-global observations of total lightning, include

explicit corrections for DE, and are available as standardized, freely accessible gridded products at spatial and temporal scales compatible with global models. However, LEO instruments sample a given region only occasionally. Obtaining robust gridded estimates of lightning density therefore generally require temporal and/or spatial smoothing to compensate for sparse sampling. Consequently, these datasets are particularly well suited to evaluating climatological spatial patterns, seasonal variability, and other relatively long-term statistics, but are less suitable for assessing the evolution of individual convective systems.

In contrast to LEO instruments, GEO lightning imagers continuously monitor a fixed portion of the Earth's surface, providing substantially higher temporal sampling and enabling observations at timescales relevant to individual convective systems. Examples include the Geostationary Lightning Mapper (GLM) on the GOES-R series over the Americas (Rudlosky *et al.*, 2019), the Lightning Mapping Imager (LMI) on China's Fengyun-4 series over eastern Asia, western Australia, and adjacent oceans (Ni *et al.*, 2021), and the Lightning Imager (LI) on Meteosat Third Generation (MTG) over Europe, Africa, and adjacent regions (Bliznák and Sokol, 2026). Like LEO optical sensors, these instruments detect total lightning without directly distinguishing between CG and IC flashes, although efforts have been made to separate the two (Ringhausen *et al.*, 2021). Their continuous observations provide new opportunities for evaluating lightning parameterizations beyond climatological spatial patterns, including the diurnal cycle and the timing and evolution of lightning associated with individual convective systems. GEO lightning observations are already being used for regional evaluations; for example, GLM observations have revealed biases in the spatial distribution and diurnal cycle of lightning simulated by CTH (Dang *et al.*, 2025). However, the DE of GEO instruments is not spatially uniform across the GEO field of view and can decrease substantially at large viewing angles and toward its edges (Murphy and Said, 2020; Wu *et al.*, 2023; Bliznák and Sokol, 2026). In addition, lightning detection is affected by variations in solar illumination associated with the day–night cycle and by the optical thickness of clouds above the lightning flashes. Differences in viewing geometry, instrument characteristics, DE, and data processing therefore need to be considered when combining observations from different geostationary sensors.

Both LEO and GEO optical lightning sensors primarily detect emissions near the 777 nm atomic oxygen line. However, observations at this wavelength do not capture all forms of electrical activity within thunderstorms. In particular, corona discharges, which comprise large numbers of streamers, produce little or no detectable emission at 777 nm and may therefore be missed by conventional space-based lightning imagers (Soler *et al.*, 2020). Instead, their optical emission is concentrated near 337 nm and is accompanied by bursts of Very High Frequency (VHF) radio emission. Space-borne observations from the Fast On-orbit Recording of Transient Events (FORTE, Jacobson and Heavner, 2005) LEO satellite and the Atmosphere–Space Interactions Monitor (ASIM, Soler *et al.*, 2020) have shown that such discharges can be detected from orbit through these optical or radio signatures. The planned Constellation of Radio Frequency Sensors (CubeSpark, Gatlin *et al.*, 2023) aims to combine optical measurements at 777 and 337 nm with VHF observations, potentially providing additional information on thunderstorm evolution beyond conventional lightning detection (Soler *et al.*, 2024).

All lightning observation systems thus have measurement and detection characteristics that can influence both the development and evaluation of parameterizations. These include differences in DE, sensor type and viewing geometry, temporal and spatial sampling, and the algorithms used to identify and group lightning signals into events, strokes, or flashes. For optical satellite

sensors, detection is affected by background illumination, cloud optical thickness, and thresholds used to distinguish lightning signals from noise or cosmic-ray events, whereas LLSs are influenced by network geometry, signal propagation, and location algorithms. Consequently, observations from different systems may differ in their spatial and temporal coverage, the types of lightning signals they detect, and their sensitivity to individual events or flashes, and are therefore not necessarily directly comparable across products. While the availability of coherent, well-characterized gridded LEO datasets has greatly facilitated the evaluation and development of lightning parameterizations, comparable multi-satellite datasets from GEO observations are an important remaining opportunity. In particular, their ability to resolve lightning at daily or sub-daily timescales could enable more direct evaluation of the physical relationships between environmental predictors and lightning activity and thus provide a stronger basis for developing and testing physically based parameterizations.

Besides the challenges inherent to observing lightning, additional issues arise when these observations are used to benchmark lightning parameterizations. When CG parameterizations such as CP_Linear, CP_Poly or CAPE×P are compared with total lightning observations from space, the predicted CG lightning is usually scaled by an estimated CG fraction within each grid-cell — e.g., derived from cold-cloud depth (Price and Rind, 1993) or latitude (Prentice and Mackerras, 1977) — which can distort evaluation metrics. The reverse problem arises when predicted total lightning is compared with ground-based observations, which often predominantly detect CG lightning. Additionally, evaluations are not always fully independent as parameterizations which were calibrated using a specific lightning product might have inherited its sampling biases during training, which can influence their apparent performance in subsequent assessments when compared to different datasets. For example, ENV_XGB achieves a spatial correlation of 0.80 in cross-validation against FLASHMAP data used for training (Krause *et al.*, accepted), but this decreases to 0.69 when evaluated against ENTLN observations from the same year. Finally, the evaluation metrics might not only reflect the performance of the parameterization itself but also the model's ability in simulating the predictor variables. For instance, the spatial correlation coefficient dropped from 0.92 to 0.77 when Verjans and Franzke (2025) applied their parameterization in a climate model compared to the reanalysis data the model was originally trained on. Given the short time period of lightning observations, evaluations are typically conducted with respect to lightning climatologies, inter-annual variability, seasonality, or the diurnal cycle rather than long-term trends, leaving the ability of models to reproduce such trends poorly constrained.

3.2 Spatial evaluation

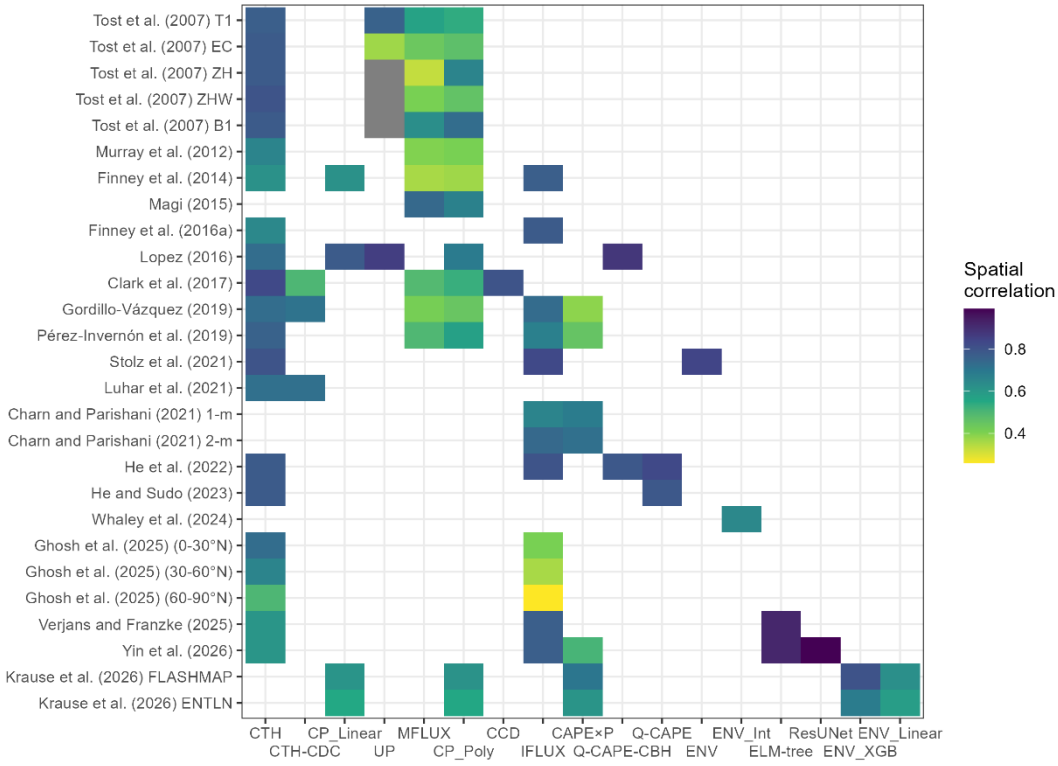
The CTH approach is still the most common lightning parameterization and is often used as a benchmark for newer schemes (Fig. 3). Maybe unsurprisingly, newly developed parameterizations usually outperform older approaches in the studies that introduce them, but their skill is less consistent when later implemented by other groups and models. Some schemes, including CTH and IFLUX, generally capture the spatial patterns of observed lightning densities well ($r > 0.7$), whereas others like MFLUX and CP_Poly perform relatively poorly ($r < 0.6$), or show mixed performance (UP, CAPE×P) (Fig. 3a). Interestingly, Tost *et al.* (2007) reported that CTH not only had the highest correlation compared to UP, MFLUX, and CP_Poly, but was also the most robust to the underlying convection scheme. However, CTH tends to overestimate spatial variability (Fig. 3b),

largely due to a strong exaggeration of the land-ocean contrast in lightning activity (Fig. 3c). In contrast, most other parameterizations, including the "aerosol variant" CTH-CDC, underestimate both spatial variability and the land-ocean contrast, even those parameterizations that use separate equations for land and ocean cells (Fig. 3b+c). Even when separate land and ocean relationships are used, the observed contrast may not be reproduced if the calibration was not specifically constrained by the respective mean flash rates. Differences between the predictor fields used for calibration and application may introduce additional biases, particularly when relationships derived from reanalysis data are applied in climate models. Moreover, observational lightning products themselves differ substantially in their land–ocean contrast, such that a parameterization calibrated against one dataset may appear biased when evaluated against another. These issues were compounded for early parameterizations by the limited observations available over maritime regions. The exceptions are Q-CAPE-CBH and ENV_Int, which reproduce the land-ocean contrast relatively well, even though ENV_Int does not separate land and ocean grid boxes.

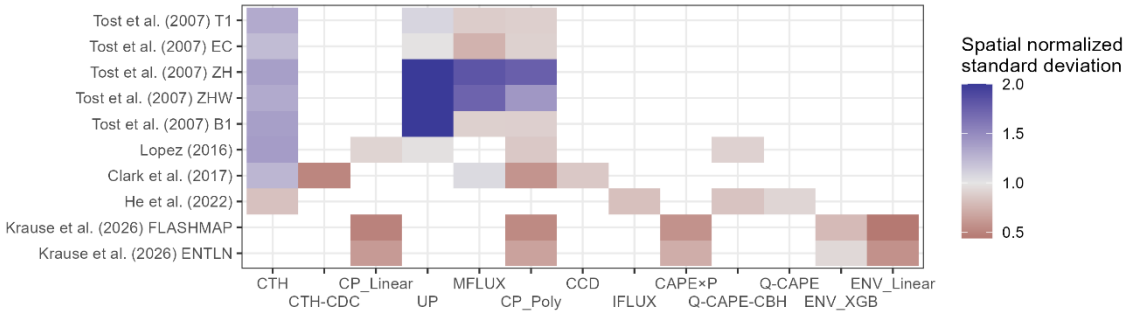
A common bias across many schemes, including CTH, is the overestimation of lightning in the tropics and underestimation in sub- and extratropical regions (Finney *et al.*, 2014; He *et al.*, 2022; Ghosh *et al.*, 2025). Within the tropics, the overestimation is particularly pronounced over the Amazon and the Maritime Continent, whereas lightning over Central Africa is underestimated by all parameterizations. While this is also the case for **CTH**, it still captures the maximum over the Congo Basin better than others (Lopez, 2016), although not all convection schemes reproduce this maximum (Tost *et al.*, 2007). CTH also underestimates lightning in Europe, Central and North America, and Argentina, while overestimating it in Amazonia, Southeast Asia, the Maritime Continent, and northern Australia (Tost *et al.*, 2007; Murray *et al.*, 2012; Finney *et al.*, 2016a; Lopez, 2016; Clark *et al.*, 2017; Verjans and Franzke, 2025; Krause *et al.*, 2014; Finney *et al.*, 2014). Additionally, it simulates too few low and high flash frequencies and too many intermediate values (Finney *et al.*, 2014; Wong *et al.*, 2013). The **UP** parameterization also overestimates lightning over the Amazon and – for some convection schemes – the oceans and underestimates it over Central Africa (Tost *et al.*, 2007; Lopez, 2016). Spatial variability is sometimes captured accurately, but for some configurations exceeds observed values by a factor of more than two (Fig. 3b). **CP_Linear** produces too much lightning over the Amazon, the Maritime Continent, and tropical oceans, while underestimating lightning over Central Africa, Northern Argentina, North America, and western India (Lopez, 2016; Finney *et al.*, 2014). However, it captures extratropical lightning better than CTH (Flemming *et al.*, 2015). **MFLUX** greatly overestimates lightning over the oceans, in particular over the western tropical Pacific, while underestimating it in the extratropics and, in particular, Central Africa (Finney *et al.*, 2014; Tost *et al.*, 2007; Murray *et al.*, 2012; Gordillo-Vázquez *et al.*, 2019; Allen and Pickering, 2002). In contrast to most other parameterizations, MFLUX tends to simulate the correct or even too low magnitude over the Amazon and the Maritime Continent (Tost *et al.*, 2007; Finney *et al.*, 2014; Murray *et al.*, 2012), which is likely related to the general underestimation of continental lightning. **CP_Poly** behaves similar to MFLUX, with overestimations over tropical oceans and tropical South America, and underestimations in Central Africa and extratropical land areas (Tost *et al.*, 2007; Murray *et al.*, 2012; Finney *et al.*, 2014; Lopez, 2016; Gordillo-Vázquez *et al.*, 2019; Clark *et al.*, 2017). **CCD** resembles CTH but with a smaller land-ocean contrast (Clark *et al.*, 2017). **IFLUX** has been used in numerous comparative studies of lightning schemes and demonstrates a

similar or better ability to predict spatial patterns as CTH (with the exception of Ghosh *et al.* (2025)). It improves the tropics-subtropics ratio in lightning activity (Finney *et al.*, 2014) but underestimates lightning in Central Africa, India, Australia, and southern US, while overestimating it over tropical oceans, the Maritime Continent, the Amazon, western North America, Central Asia, and boreal regions (Finney *et al.*, 2016a; Stolz *et al.*, 2021; Charn and Parishani, 2021; He *et al.*, 2022; Verjans and Franzke, 2025; Finney *et al.*, 2014). The **CAPE×P** approach, initially shown to be an excellent predictor for lightning in the continental US (Romps *et al.*, 2014), clearly loses skill at global scale, despite a high correlation between lightning and CAPE times precipitation over land (Romps *et al.*, 2018). This might be related to using the same equation for land and ocean grid boxes (note that Charn and Parishani (2021) applied separate scaling factors over land and oceans, which likely explains the higher correlation relative to other studies shown in Fig. 3a). CAPE×P overestimates lightning particularly over tropical oceans (Romps *et al.*, 2018; Yin *et al.*, 2026), but also over the Amazon and Southeast Asia, while underestimating it in mid-latitude land areas and also over mid-latitude oceanic regions east of the continents (Gordillo-Vázquez *et al.*, 2019; Charn and Parishani, 2021; Pérez-Invernón *et al.*, 2019). **CMF-T** captures the general spatial distribution of lightning but overestimates lightning activity over the Amazon and underestimates it over Central Africa. It also underestimates lightning activity over oceanic regions downwind of continents while overestimating it over remote tropical ocean regions (Liaskos *et al.*, 2015). **Q-CAPE-CBH** improves lightning distribution in South Asia, the US, and over the oceans relative to CTH, but underestimates lightning particularly in Central Africa and also in Colombia, Ural Mountains, and some ocean regions near continents (Lopez, 2016; He *et al.*, 2022). The Central African underestimation also occurs in the modified **Q-CAPE** scheme (He *et al.*, 2022). **ENV** produces too much lightning over tropical oceans and too little over (sub)tropical land (Stolz *et al.*, 2021). **ENV_Int** overestimates lightning over the western coasts of North and South America, mountains, South Africa, and Australia, while underestimating it over the eastern half of North and South America, India, Central and North Africa (Whaley *et al.*, 2024). **ELM-tree** substantially reduces the Central African bias but still overestimates tropical ocean and eastern African lightning, while underestimating it in Southeastern South America and North America (Verjans and Franzke, 2025). **ResUNet** captures spatial patterns even better and avoids the overestimation of ELM-tree over tropical oceans, but underestimates lightning in high latitudes (Yin *et al.*, 2026). **ENV_XGB** reproduces the general contrast in lightning activity between tropical and extratropical regions, including the pronounced maximum over Central Africa, but overestimates lightning activity over the Amazon (Krause *et al.*, accepted). In contrast, **ENV_Linear** underestimates lightning activity in the tropics and overestimates it at higher latitudes (Krause *et al.*, accepted).

a


Tost et al. (2007) T1
Tost et al. (2007) EC
Tost et al. (2007) ZH
Tost et al. (2007) ZHW
Tost et al. (2007) B1
Murray et al. (2012)
Finney et al. (2014)
Magi (2015)
Finney et al. (2016a)
Lopez (2016)
Clark et al. (2017)
Gordillo-Vázquez (2019)
Pérez-Invernón et al. (2019)
Stolz et al. (2021)
Luhar et al. (2021)
Charn and Parishani (2021) 1-m
Charn and Parishani (2021) 2-m
He et al. (2022)
He and Sudo (2023)
Whaley et al. (2024)
Ghosh et al. (2025) (0-30°N)
Ghosh et al. (2025) (30-60°N)
Ghosh et al. (2025) (60-90°N)
Verjans and Franzke (2025)
Yin et al. (2026)
Krause et al. (2026) FLASHMAP
Krause et al. (2026) ENTLN
CTH
CTH-CDC
CP_Linear
UP
MFLUX
CP_Poly
CCD
IFLUX
CAPE×P
Q-CAPE-CBH
Q-CAPE
ENV
ENV_Int
ELM-tree
ResUNet
ENV_XGB
ENV_Linear
Spatial correlation
0.8
0.6
0.4

b


Tost et al. (2007) T1
Tost et al. (2007) EC
Tost et al. (2007) ZH
Tost et al. (2007) ZHW
Tost et al. (2007) B1
Lopez (2016)
Clark et al. (2017)
He et al. (2022)
Krause et al. (2026) FLASHMAP
Krause et al. (2026) ENTLN
CTH
CTH-CDC
CP_Linear
UP
MFLUX
CP_Poly
CCD
IFLUX
CAPE×P
Q-CAPE-CBH
Q-CAPE
ENV_XGB
ENV_Linear
Spatial normalized standard deviation
2.0
1.5
1.0
0.5

c

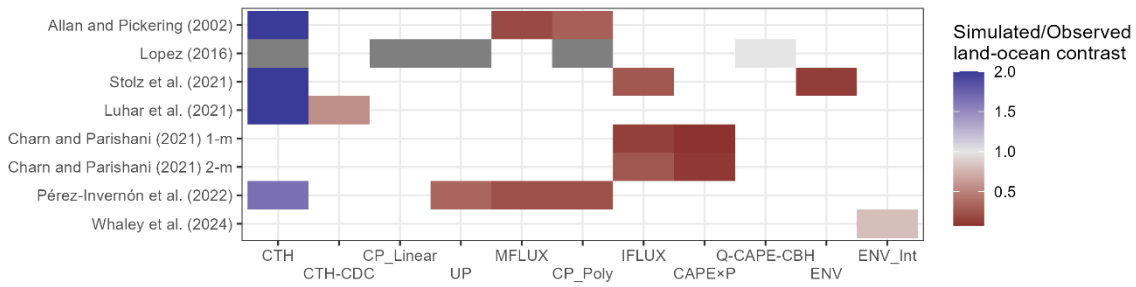

Allan and Pickering (2002)
Lopez (2016)
Stolz et al. (2021)
Luhar et al. (2021)
Charn and Parishani (2021) 1-m
Charn and Parishani (2021) 2-m
Pérez-Invernón et al. (2022)
Whaley et al. (2024)
CTH
CTH-CDC
CP_Linear
UP
MFLUX
CP_Poly
IFLUX
CAPE×P
Q-CAPE-CBH
ENV
ENV_Int
Simulated/Observed land-ocean contrast
2.0
1.5
1.0
0.5

Figure 3: Evaluation of different lightning parameterizations in reproducing the spatial patterns of observed lightning climatologies as extracted from the literature. Panels show: (a) correlation, (b) normalized standard deviation, and (c) land-ocean contrast relative to observations (capped at 2.0 to enhance visibility). Higher values in a) indicate better reproduction of mean lightning spatial patterns. Blue colours in b) indicate overestimation of spatial variability, while red indicates underestimation. Similarly, blue colours in c) indicate overestimation of the land-ocean contrast in lightning activity. Note that evaluation methods differ across studies (e.g. Clark *et al.* (2017) evaluated against LIS/OTD observations within ±38°, whereas Tost *et al.* (2007) used ±60°, see Table S2) so direct comparison across studies should be made cautiously. The abbreviations T1, EC, ZH, ZHW, and B1 in Tost *et al.* (2007) denote different convection schemes. In Charn and Parishani (2021), the labels 1-m and 2-m refer to one-moment and two-moment microphysics schemes, respectively. The number of moments indicates the degrees of freedom used to represent the size distribution of precipitating hydrometeors. Murray *et al.* (2012) included a seasonal dimension, reflecting spatiotemporal performance. Some values were estimated from graphs (https://plotdigitizer.com/app) when not directly reported. Grey boxes show parameterizations included in the comparison but with unknown values because symbols fell outside the plotting range. The individual values for each study and parameterization can be extracted from Table S2.

3.3 Temporal evaluation

Most temporal evaluations of lightning parameterizations have focused on the seasonal cycle, while the diurnal cycle and inter-annual variability have received less attention (Fig. 4).

Seasonal cycle: Lightning activity generally follows the shift of the intertropical convergence zone, resulting in peak global lightning activity during Northern Hemisphere (NH) summer, as lightning is concentrated over land areas. Consequently, the parameterizations' ability to reproduce lightning seasonality depends on two key factors: (1) their ability to simulate the land-ocean contrast, which is facilitated by the use of separate equations for land and ocean grid boxes — and (2) their ability to capture the seasonality of the predictor variable. All parameterizations struggle to reproduce the observed annual cycle of global lightning, with sometimes even negative correlations (Fig. 4a). Correlations improve when evaluations are conducted for each hemisphere individually, especially when the observations include extratropical regions (i.e. are not only based on TRMM LIS). However, even for these cases the amplitude of the seasonal cycle is typically underestimated, at least for the NH (Fig. 4b). Noteworthy, many parameterizations simulate a secondary maximum during NH winter when global lightning activity according to LIS/OTD is low (Gordillo-Vázquez *et al.*, 2019; Tost *et al.*, 2007). The **CTH** approach generally captures the month of peak lightning in most regions, apart from Equatorial South America and parts of South Asia (Krause *et al.*, 2014). Timing accuracy varies: while Tost *et al.* (2007) reported that CTH simulates the boreal summer maximum about 20 days too early, Stolz *et al.* (2021) found a delay of two months. CTH-CDC also captures seasonality in most tropical regions, apart from NH South America (Clark *et al.*, 2017). **CP_Linear** simulates the maximum roughly one month too late (Finney *et al.*, 2014). **UP** has great difficulties to simulate the seasonal cycle and shows high variability across different convection schemes (Tost *et al.*, 2007). Allen and Pickering (2002) found that **MFLUX** represented the 1996 seasonal cycle more accurately than CTH and **CP_Poly**. In contrast, Tost *et al.* (2007) reported that neither MFLUX nor CP_Poly captured the seasonal cycle of global lightning activity, while Gordillo-Vázquez *et al.* (2019) noted that MFLUX performed better than

CP_Poly. **IFLUX** captures seasonality reasonably well but typically peaks 1-2 months later than observed (Finney *et al.*, 2014; Gordillo-Vázquez *et al.*, 2019; Stolz *et al.*, 2021). **CAPE×P**'s global lightning activity tends to peak about one month earlier than observed and also overestimates global lightning occurrence during the NH winter (Gordillo-Vázquez *et al.*, 2019). At the hemispheric scale, however, a delayed peak and an overestimation of seasonal variability have been reported (Yin *et al.*, 2026). **ENV** predicts the peak in both hemispheres two months too late (Stolz *et al.*, 2021), while **ELM-tree** and **ResUNet** simulate the seasonal cycle in LIS/OTD very accurately (Verjans and Franzke, 2025; Yin *et al.*, 2026). **ENV_XGB** reproduces the seasonal cycle observed in FLASHMAP during 2019 well, particularly at the hemispheric scale (Krause *et al.*, accepted). **ENV_Linear** also captures the timing but underestimated the magnitude of the seasonal cycle at the hemispheric scale (Krause *et al.*, accepted).

Inter-annual variability: Wang *et al.* (2025) compared the global inter-annual variability simulated by **CTH** with observations from WWLLN and Schumann Resonance measurements over 2013–2021. They found that CTH did not capture the observed variability and instead produced a significant increasing trend, while also noting that the observational products themselves do not always agree on the magnitude and direction of annual anomalies. Verjans and Franzke (2025) and Yin *et al.* (2026) both evaluated inter-annual variability using a common set of six test years, selected from a 27-year period of LIS/OTD observations (with lightning data only partly available for some years). They reported good prediction skill for **IFLUX**, **ELM-tree**, and **ResUNet**, especially for the NH, while CTH and **CAPE×P** performed worse (Fig. 4). However, spatial and temporal coverage differs among these years, introducing apparent year-to-year variability that does not reflect actual changes in lightning activity. Krause and Rammig (submitted) showed that the reported positive correlations disappear for all parameterizations when the analysis is restricted to consistent spatiotemporal coverage. This may reflect limitations of the parameterizations, but could also be related to limitations of the observational record, including the small number of test years, restricted spatial coverage (±38°), temporal smoothing, and the observations assembled from three separate lightning missions.

Time-series: Time-series evaluations combine seasonality and inter-annual variability. Clark *et al.* (2017), analysing five parameterizations, found that only the **CTH-CDC** approach reproduced the observed temporal variability in LIS/OTD observations during 1996–2008 within ±38° to some extent (Fig. 4), but given its poor spatial performance pointed out that this may result from error cancellation across regions. In contrast, Krause *et al.* (accepted) found a positive correlation for five CG parameterizations when evaluating monthly time-series against ENTLN observations for 2015–2018. This difference may partly be explained by the inclusion of mid- and high-latitude regions in their analysis, which pronounces the seasonal cycle in global lightning activity. Correlations increased further when monthly lightning activity was aggregated at the hemispheric scale, although all parameterizations except **ENV_XGB** underestimated the magnitude of the observed variability.

Diurnal cycle: Only one study has compared multiple parameterizations against the observed diurnal cycle of global lightning (Tost *et al.*, 2007; Fig. 4). Locally, lightning activity over land areas usually peaks in the late afternoon. The **CTH** scheme captures the first global maximum at 14:00 UTC (corresponding to the African afternoon peak), but underestimates the second

maximum in the Americas. **CP_Poly** reproduces the general diurnal pattern but also fails to capture the second maximum. The performance of **UP** and **MFLUX** is overall worse and depends more on the convection scheme (Tost *et al.*, 2007).

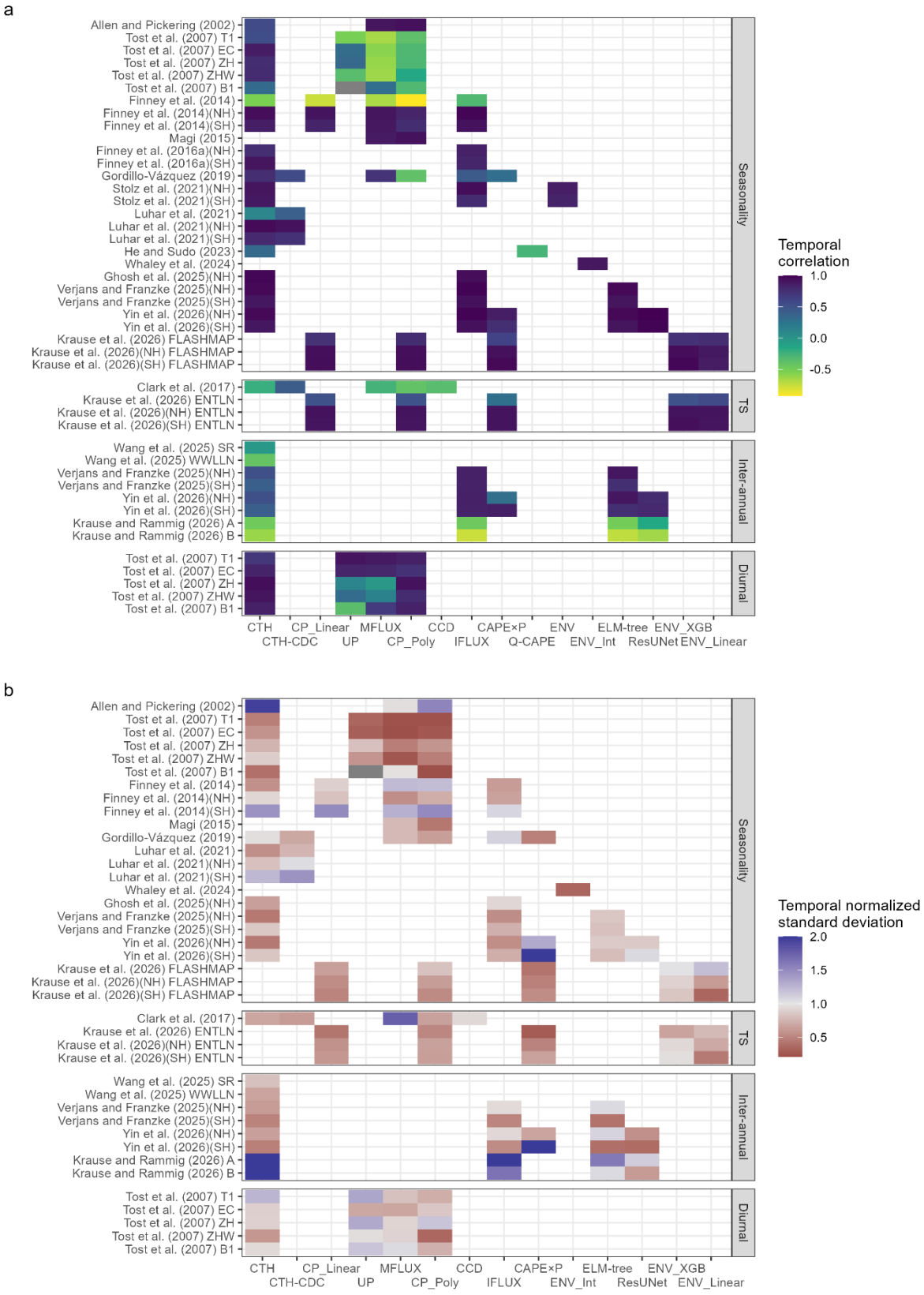

a
Allen and Pickering (2002)
Tost et al. (2007) T1
Tost et al. (2007) EC
Tost et al. (2007) ZH
Tost et al. (2007) ZHW
Tost et al. (2007) B1
Finney et al. (2014)
Finney et al. (2014)(NH)
Finney et al. (2014)(SH)
Magi (2015)
Finney et al. (2016a)(NH)
Finney et al. (2016a)(SH)
Gordillo-Vázquez (2019)
Stolz et al. (2021)(NH)
Stolz et al. (2021)(SH)
Luhar et al. (2021)
Luhar et al. (2021)(NH)
Luhar et al. (2021)(SH)
He and Sudo (2023)
Whaley et al. (2024)
Ghosh et al. (2025)(NH)
Verjans and Franzke (2025)(NH)
Verjans and Franzke (2025)(SH)
Yin et al. (2026)(NH)
Yin et al. (2026)(SH)
Krause et al. (2026) FLASHMAP
Krause et al. (2026)(NH) FLASHMAP
Krause et al. (2026)(SH) FLASHMAP
Clark et al. (2017)
Krause et al. (2026) ENTLN
Krause et al. (2026)(NH) ENTLN
Krause et al. (2026)(SH) ENTLN
Wang et al. (2025) SR
Wang et al. (2025) WWLLN
Verjans and Franzke (2025)(NH)
Verjans and Franzke (2025)(SH)
Yin et al. (2026)(NH)
Yin et al. (2026)(SH)
Krause and Rammig (2026) A
Krause and Rammig (2026) B
Tost et al. (2007) T1
Tost et al. (2007) EC
Tost et al. (2007) ZH
Tost et al. (2007) ZHW
Tost et al. (2007) B1
Seasonality
TS
Inter-annual
Diurnal
CTH
CTH-CDC
CP_Linear
UP
MFLUX
CP_Poly
CCD
IFLUX
CAPE×P
Q-CAPE
ENV
ENV_Int
ELM-tree
ResUNet
ENV_XGB
ENV_Linear
Temporal correlation
1.0
0.5
0.0
-0.5
b
Allen and Pickering (2002)
Tost et al. (2007) T1
Tost et al. (2007) EC
Tost et al. (2007) ZH
Tost et al. (2007) ZHW
Tost et al. (2007) B1
Finney et al. (2014)
Finney et al. (2014)(NH)
Finney et al. (2014)(SH)
Magi (2015)
Gordillo-Vázquez (2019)
Luhar et al. (2021)
Luhar et al. (2021)(NH)
Luhar et al. (2021)(SH)
Whaley et al. (2024)
Ghosh et al. (2025)(NH)
Verjans and Franzke (2025)(NH)
Verjans and Franzke (2025)(SH)
Yin et al. (2026)(NH)
Yin et al. (2026)(SH)
Krause et al. (2026) FLASHMAP
Krause et al. (2026)(NH) FLASHMAP
Krause et al. (2026)(SH) FLASHMAP
Clark et al. (2017)
Krause et al. (2026) ENTLN
Krause et al. (2026)(NH) ENTLN
Krause et al. (2026)(SH) ENTLN
Wang et al. (2025) SR
Wang et al. (2025) WWLLN
Verjans and Franzke (2025)(NH)
Verjans and Franzke (2025)(SH)
Yin et al. (2026)(NH)
Yin et al. (2026)(SH)
Krause and Rammig (2026) A
Krause and Rammig (2026) B
Tost et al. (2007) T1
Tost et al. (2007) EC
Tost et al. (2007) ZH
Tost et al. (2007) ZHW
Tost et al. (2007) B1
Seasonality
TS
Inter-annual
Diurnal
CTH
CTH-CDC
CP_Linear
UP
MFLUX
CP_Poly
CCD
IFLUX
CAPE×P
ENV_Int
ELM-tree
ResUNet
ENV_XGB
ENV_Linear
Temporal normalized standard deviation
2.0
1.5
1.0
0.5

Figure 4: Assessment of different lightning parameterizations in reproducing temporal variations of observed lightning across multiple time scales: seasonal, time-series (TS), inter-annual, and diurnal. Some studies split the evaluation between Northern Hemisphere (NH) and Southern Hemisphere (SH). In panel (a), darker colours in the correlation indicate better performance in capturing the timing of lightning activity. In panel (b), blue shades in the normalized standard deviation represent overestimation (capped at 2.0), while red shades indicate underestimation of the amplitude of variations. The abbreviations A and B in Krause and Rammig (submitted) refer to two different approaches for ensuring temporal consistency: in A, the incomplete year 2023 was excluded, whereas in B, October-December was excluded from all six years. The individual values for each study and parameterization can be extracted from Table S3.

3.4 Reliability beyond statistical metrics

Being able to reproduce observed lightning patterns is a necessary but not sufficient condition for making reliable lightning projections under novel climate conditions. The fact that most parameterizations require separate equations for land and ocean further suggests that important processes or variables are still not adequately represented. Recently, data-driven machine learning approaches achieved impressive statistical performance when evaluated against observations, with the test years explicitly excluded from the training data (Verjans and Franzke, 2025; Yin *et al.*, 2026). For instance, Verjans and Franzke (2025) reported that ELM-tree explained 72% of the variance in daily LIS/OTD lightning observations, while Yin *et al.* (2026) reported 89% for ResUNet. However, such high evaluation scores do not necessarily demonstrate that these highly flexible models have learned transferable relationships between atmospheric conditions and lightning activity.

Krause and Rammig (submitted) showed that an even higher predictive skill can be achieved without using any meteorological predictors. Specifically, a simple climatological benchmark was constructed by calculating the mean daily lightning density for each grid-cell and calendar day of the year across all training years. These climatological means were then used to predict lightning density in the corresponding grid-cells and calendar days of the test years, irrespective of the actual meteorological conditions. In other words, the benchmark reproduces the mean spatial distribution and seasonal cycle of lightning but cannot capture year-to-year variations in lightning activity. Despite its simplicity, this benchmark explained 92% of the variance in daily LIS/OTD lightning observations in the test years and also reproduced spatial patterns and hemispheric seasonal cycles with performance comparable to or better than the much more complex machine-learning models. This demonstrates that, for strongly smoothed lightning products such as LIS/OTD, test observations are already highly predictable from the spatiotemporal climatology contained in the training data. This issue may be particularly important for convolutional neural networks and other approaches that receive information from other grid-cells, because recurring large-scale spatial patterns in predictor fields can provide implicit information about location and season. Such models could learn to reconstruct recurring training data patterns without being appropriately sensitive to changes in meteorological drivers. Evaluating machine-learning lightning models for climate projections therefore requires tests that go beyond conventional spatial and seasonal skill metrics and explicitly assess whether their responses to changing environmental conditions are physically meaningful and transferable beyond the climate represented in the training data (Krause and Rammig, submitted).

Among the traditional parameterizations, ice-based schemes like IFLUX and Q-CAPE are generally considered to have the strongest physical connection to lightning generation because they explicitly represent the microphysical charging processes occurring within thunderstorms (Cheng, 2021). These schemes more directly capture the collisions between graupel, snow, and ice crystals in mixed-phase cloud regions where electrification occurs. However, uncertainties remain in how models simulate cloud microphysics, as well as in the evaluation of simulated ice fluxes, because the concentration of ice particles in clouds is difficult to observe (Ghosh *et al.*, 2025). Convective intensity approaches such as CAPE×P also have a relatively strong physical basis because strong updrafts play a critical role in transporting and separating charged ice particles within deep convective clouds. In contrast, size-based parameterizations such as CTH are more empirical and only indirectly linked to the charging process. Although larger and deeper storms tend to produce more lightning, these schemes mainly rely on statistical relationships and do not explicitly represent the underlying cloud microphysics responsible for electrification.

4 Lightning projections

4.1 Global sensitivity

The CTH approach is by far the most common one to project changes in lightning activity (Fig. 5). Most studies looked at total lightning, while projections on CG lightning are rare and in some cases it is not even clear which of both was reported. Whether CG lightning responds more strongly to climate change than total lightning is uncertain as the few studies that reported changes for both lightning types (all computing CG lightning from CTH-derived total lightning multiplied by the CCD-derived CG fraction) came to different conclusions: Price and Rind (1994c) reported a 30% increase in total lightning and noted that the increase was larger for CG lightning. However, in a follow-up paper they referred to a 30% increase in CG lightning (Price and Rind, 1994a). Two other studies found that CG lightning was roughly 33% less sensitive to climate change than total lightning (Pérez-Invernón *et al.*, 2023; Krause *et al.*, 2014). Several studies did not report changes in lightning flash frequency but instead changes in lightning NO_X production. While older studies often assumed CG lightning to be much more potent in generating NO_X than intra-cloud lightning (Price *et al.*, 1997), recent research suggests their NO_X production efficiency are similar (He *et al.*, 2022). Depending on this assumption, changes in NO_X production are thus rather indicative for changes in CG lightning or total lightning. Averaged over all three variables (total lightning, CG lightning, lightning NO_X production) and parameterizations (i.e. one mean value per parameterization), lightning increases by 5.5±8.7% per degree global warming. Averaged over all projections the lightning sensitivity is higher at 7.7±8.3% K^{-1}. This is due to the large overrepresentation of CTH, with 59% of the projections applying CTH. Interestingly, the **CTH** approach yields relatively similar lightning sensitivities in different climate models and scenarios (9.4±6.1% K^{-1}), despite the fifth-power relationship making lightning very sensitive to simulated changes in cloud height. This apparent consistency may partly reflect the relatively robust response of tropopause height to warming (Santer *et al.*, 2003), which may contribute to similarities in projected changes in CTH, particularly in the tropics. There is one outlier by Lamarque *et al.* (2005) that has the highest lightning sensitivity across all projections (~44% K^{-1}), however note that the associated global temperature increase was not reported and had to be estimated

(Schumann and Huntrieser (2007) computed an even higher value of 60% K^{-1} but their assumed 2000-2100 temperature increase of 2 K seems too low for the A2 scenario). Conversely, one model using CTH simulates a decrease in lightning NO_X, but no baseline value was reported (Thornhill *et al.*, 2021). Assuming a baseline of 5 Tg N yr^{-1} yields a sensitivity of -0.58% K^{-1}. The variant of CTH, **CTH-CDC**, has a substantially lower sensitivity (3.4±4.7% K^{-1}). **UP**, **CP_Poly**, and **CCD** have similar sensitivities (2.8% K^{-1}, 2.2±3.1% K^{-1} and 3.2±0.7% K^{-1}, respectively), but all of these are based on only one model. Despite being closely related to CTH, CCD responds less strongly to warming because the rising freezing level partly offsets increases in CTH. Consequently, CCD changes relatively little even when CTH increases, explaining the substantially weaker lightning response of CCD compared with CTH-based parameterizations (Clark *et al.*, 2017). **MFLUX** has a negative sensitivity (-3.5±6.8% K^{-1}), including the lowest value across all projections (-11% K^{-1}; Finney *et al.*, 2016b). The original **IFLUX** parameterization also predicts a decrease in lightning frequency under warming (-4.5±3.9% K^{-1}), (Finney *et al.*, 2018) but its variant, **IFLUX_T**, on average assumes a slight increase (0.8±4.7% K^{-1}). (Note that 4/6 IFLUX_T projections are from Charn and Parishani (2021) who scaled land and ocean lightning to match LIS/OTD; as ocean lightning in their study increased more than land lightning this reduced the projected increase in global lightning). **CAPE×P** has a sensitivity of 3.7±2.7% K^{-1}. Again, this value is based on simulations from a single climate model and the uncertainty in this case chiefly arises from how CAPE is computed (Charn and Parishani, 2021). Also note that the frequently cited sensitivity of 12% K^{-1} applies only to the contiguous US (Romps *et al.*, 2014). **Q-CAPE-CBH** has a high sensitivity of 24.2±15.6% K^{-1}, including one of the highest values across all projections (35% K^{-1}), however, this is solely based on short-term projections (2001-2020) from one model and may be subject to substantial inter-annual variability (He *et al.*, 2022). **Q-CAPE** has a value of 13.6±11.5% K^{-1}, with three out of four projections from a single model and for the historical period. **ENV_Int** and **ELM-tree** (apparently using more predictors than in the original parameterization) are almost insensitive (0.09±0.2% K^{-1} and 1.6% K^{-1}, respectively) but once again lack robustness as only having been applied in one model (Whaley *et al.*, 2024; Verjans *et al.*, 2025). **ENV_XGB** exhibits a very high sensitivity of 23.7±9.8% K^{-1}, with substantially greater sensitivity under future than historical climate conditions. In contrast, **ENV_Linear**, despite using the same predictors, exhibits a sensitivity of only 2.1±0.7% K^{-1}, highlighting the importance of not only predictor selection but also the underlying statistical modelling approach (Krause *et al.*, accepted). No projections are presently available from **CP_Linear**, **CMF-T**, **ENV**, and **ResUNet**.

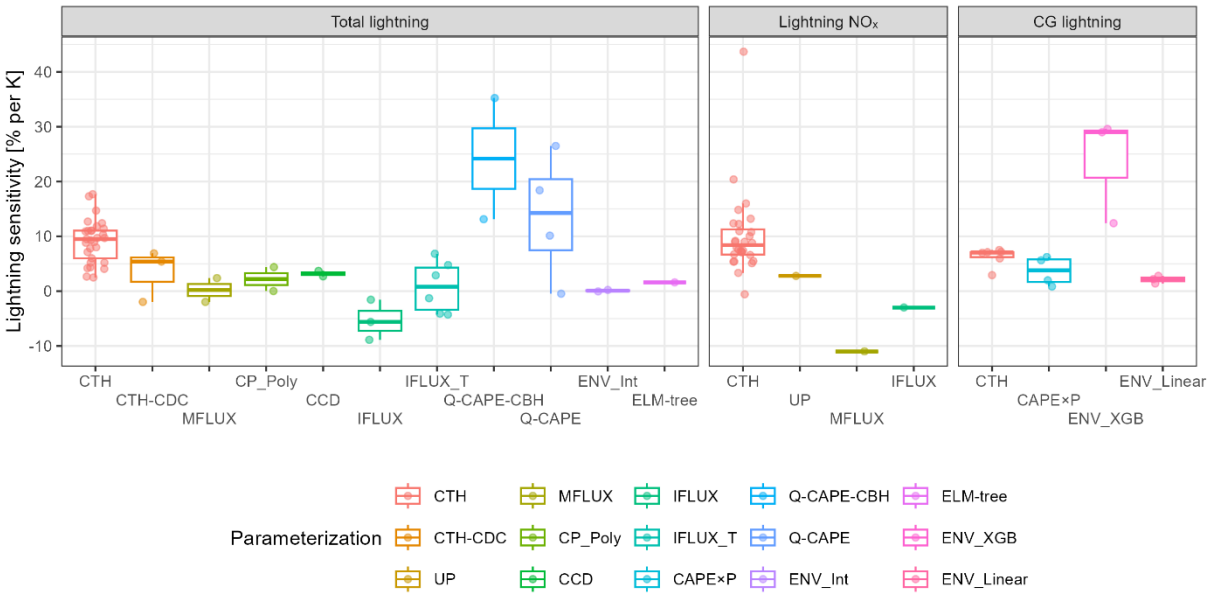


Figure 5: Change in global lightning frequency per degree global warming for different lightning parameterizations. If a study conducted multiple projections for the same parameterization (e.g. using different model setups or emission scenarios) each projection is plotted separately. The individual values for each projection can be extracted from Table S4.

4.2 Spatial patterns of projected lightning changes

At regional scale, lightning projections tend to increase more in high latitudes relative to the tropics, where some parameterizations assume decreasing lightning activity. This contradicts earlier observation-based findings that lightning in the tropics reacts much more sensitive to changes in wet bulb temperature (Williams, 1994) but supports the findings of Reeve and Toumi (1999) who found no correlation between lightning and temperature in the tropics. The **CTH** approach generally projects larger increases over land than over the oceans where lightning in some models decreases (Price and Rind, 1994c; Krause *et al.*, 2014; Clark *et al.*, 2017; Finney *et al.*, 2016b). Over land, decreases are sometimes projected over Northeastern South America, while increases are simulated for Central Africa, the Maritime Continent, and in high latitudes (Price and Rind, 1994c; Krause *et al.*, 2014; Pérez-Invernón *et al.*, 2023; Finney *et al.*, 2016b; Guryanov *et al.*, 2024). **UP** projects increases in the Eastern US and Russia but decreases in Africa and Australia (Finney *et al.*, 2016b). **MFLUX** results in larger increases (or less decreases) over land than over the ocean, while for **CTH-CDC**, **CP_Poly**, and **CCD** this depends on the emission scenario (Clark *et al.*, 2017). Over land, lightning decreases under **MFLUX** mainly occur in the (sub)tropics, while increases are found in northern Asia (Finney *et al.*, 2016b). **IFLUX** also projects lightning decreases in the tropics but increases or non-significant changes in mid and high latitudes (Finney *et al.*, 2018). For **IFLUX_T**, Charn and Parishani (2021) showed large decreases in future lightning almost everywhere on Earth when using a 1-moment microphysics scheme, while the picture looked heterogeneous for a more complex, 2-moment scheme. For the latter, lightning decreased over most of Africa, Southern

Europe, the Middle East, India, and Australia but increased over most of the Americas, Eastern Europe, Russia, China, and the Maritime Continent. Under both microphysics schemes the increase (decrease) was higher (lower) over the oceans than over land (Charn and Parishani, 2021). For **CAPE×P**, global projections are only available from the same study which, however, not only tested the effect of a 1-moment vs. 2-moment microphysics scheme but also two alternative ways to compute CAPE (Charn and Parishani, 2021). These simulations suggest increasing lightning over the Maritime Continent, the oceans, and in mid and high latitudes, decreasing lightning in subtropical Africa, and contrasting projections in Central Africa and tropical South America depending on the model setup. These global modelling outcomes are broadly consistent with regional CAPE×P projections over the contiguous US (Romps *et al.*, 2014; Romps, 2019), Germany (Brisson *et al.*, 2021), the Arctic (Chen *et al.*, 2021), and the tropical ocean (Romps, 2019). Interestingly, the cloud-resolving simulations by Romps (2019) revealed the same increase for CAPE×P and IFLUX_T in the US, but a very different response over the tropical ocean (increase vs. decrease). Charn and Parishani (2021), comparing the same two parameterizations, also noted large differences under the 1-moment scheme but found that both approaches are broadly in agreement (lightning decreasing over Africa but increasing in high latitudes and over the oceans) when using the more complex 2-moment scheme. **Q-CAPE** with prognostic graupel projects increases in Eastern Africa and most of the Americas, Eurasia, and the oceans, but decreases over most of Australia and other parts of Africa (Michibata, 2024). **ENV_Int** predicts more lightning in mid-latitudes, particularly in Siberia, the western US, and Australia (Whaley *et al.*, 2024). In contrast, lightning is projected to decrease over tropical land and the Arctic. **ELM-tree** projects increases in Eastern Africa, East and Southeast Asia, Eastern North America, and southern South America, and decreases in the Amazon, Central America, and the Maritime Continent (Verjans *et al.*, 2025). **ENV_XGB** projects the largest relative increases in lightning activity at high latitudes, but also predicts substantial increases in the tropics. In contrast, **ENV_Linear** projects decreases in parts of the tropics, particularly tropical South America, alongside increases at high latitudes (Krause *et al.*, accepted).

5 Conclusions and outlook

Many parameterizations have been developed to simulate lightning in global chemistry-climate models and to project how lightning activity might change in a warmer world. CTH and IFLUX capture spatial patterns of present-day lightning activity relatively well, while MFLUX, CAPE×P, and convective precipitation-based approaches typically perform worse. Some newer approaches, such as Q-CAPE-CBH and Q-CAPE, have also shown promising results, but they need to be confirmed by other studies. Machine-learning approaches have recently achieved remarkably high evaluation scores, but assessing their predictive skill may require more targeted tests beyond standard evaluation metrics (Krause and Rammig, submitted). Simulating the magnitude of spatial and temporal variability remains challenging and is typically underestimated by parameterizations. Capturing inter-annual variability may provide a particularly useful test of a parameterization's suitability for future projections, yet this aspect has received limited attention, and the studies conducted so far indicate that existing parameterizations struggle to reproduce observed year-to-year variations (Wang *et al.*, 2025; Krause and Rammig, submitted).

CTH, CAPE×P, and IFLUX are currently the most popular approaches, however, there is a lack of consensus across parameterizations about how lightning responses to climate change. In particular, convection- versus cloud-ice-driven parameterizations predict opposite trends, as atmospheric instability and convection strength are expected to increase whereas cloud ice is expected to decrease (Romps, 2019). Additionally, even if a parameterization in principle captures the key factors influencing lightning, the accuracy of climate model projections depends on the ability to realistically simulate deep convection. While advances in computational capacity, such as cloud-resolved simulations for specific regions (Finney *et al.*, 2020; Brisson *et al.*, 2021; Kahraman *et al.*, 2022; Kawazoe *et al.*, 2025), hold promise for improving the representation of lightning in models, current computational resources are insufficient for global, century-scale simulations.

In the meantime, extending existing lightning observations by new products from GEO satellites and ground-based LLSs will provide new opportunities to evaluate lightning parameterizations. The higher temporal resolution of these new products could also allow changes in total lightning to be separated into changes in the frequency of lightning-producing events and changes in lightning intensity, for example by considering the number of lightning-producing days or hours and the amount of lightning produced during these events (Finney *et al.*, 2020). Such a decomposition could provide a more physically interpretable basis for assessing projected changes, as lightning intensity may be more directly related to thermodynamic and boundary-layer conditions, whereas the frequency of lightning-producing events may additionally depend on synoptic weather patterns and changes in atmospheric circulation. Together, these observational constraints could help identify the physical mechanisms underlying projected changes and thereby provide a basis for assessing confidence in different approaches to predicting lightning under future climate conditions.

Code and data availability

No new data was generated in this research. Identified modelling studies, evaluation scores, and lightning sensitivities can be found in files S1-S4.

Supplement link

The link to the supplement will be included by Copernicus, if applicable.

Author contributions

AK led the analysis and wrote the first manuscript draft. All authors contributed to the writing and discussion.

Competing interests

The authors declare that none of the authors has any competing interests.

Disclaimer

Copernicus Publications adds a standard disclaimer: "Copernicus Publications remains neutral with regard to jurisdictional claims made in the text, published maps, institutional affiliations, or any other geographical representation in this paper. While Copernicus Publications makes every effort to include appropriate place names, the final responsibility lies with the authors. Views expressed in the text are those of the authors and do not necessarily reflect the views of the publisher."
Please feel free to add disclaimer text at your choice, if applicable.

Acknowledgements

We thank Declan Finney, David Romps, and one anonymous reviewer for their feedback. We used ChatGPT to improve the wording and clarity of selected sections of the manuscript.

Financial support

This work was funded by Deutsche Forschungsgemeinschaft (German Research Foundation) via the FlashForest project (flashforest.eu; project number 536753546).

Review statement

The review statement will be added by Copernicus Publications listing the handling editor as well as all contributing referees according to their status anonymous or identified.

References

Abbott T H, Jeevanjee N, Cheng K Y, Zhou L J and Harris L 2025 The Land-Ocean Contrast in Deep Convective Intensity in a Global Storm-Resolving Model *J Adv Model Earth Sy* **17**. doi:10.1029/2024MS004467

Allen D, Pickering K, Duncan B and Damon M 2010 Impact of lightning NO emissions on North American photochemistry as determined using the Global Modeling Initiative (GMI) model *J Geophys Res-Atmos* **115**. doi:10.1029/2010jd014062

Allen D, Pickering K, Stenchikov G, Thompson A and Kondo Y 2000 A three-dimensional total odd nitrogen (NOy) simulation during SONEX using a stretched-grid chemical transport model *J Geophys Res-Atmos* **105** 3851-76. doi:10.1029/1999jd901029

Allen D J and Pickering K E 2002 Evaluation of lightning flash rate parameterizations for use in a global chemical transport model *J Geophys Res-Atmos* **107**. doi:10.1029/2002jd002066

Bandholnopparat K, Sato M, Adachi T, Ushio T and Takahashi Y 2020 Estimation of the IC to CG Ratio Using JEM-GLIMS and Ground-Based Lightning Network Data *J Geophys Res-Atmos* **125**. doi:10.1029/2019JD032195

Blakeslee R J, Lang T J, Koshak W J, Buechler D, Gatlin P, Mach D M, Stano G T, Virts K S, Walker T D, Cecil D J, Ellett W, Goodman S J, Harrison S, Hawkins D L, Heumesser M, Lin H, Maskey M, Schultz C J, Stewart M, Bateman M, Chanrion O and Christian H 2020 Three Years of the Lightning Imaging Sensor Onboard the International Space Station: Expanded Global Coverage and Enhanced Applications *J Geophys Res-Atmos* **125**. doi:10.1029/2020JD032918

Bliznák V and Sokol Z 2026 First validation of the Lightning Imager aboard Meteosat Third Generation satellite with Earth Networks Total Lightning Network *Int J Appl Earth Obs* **147**. doi:10.1016/j.jag.2026.105205

Boccippio D J 2002 Lightning scaling relations revisited *J Atmos Sci* **59** 1086-104. doi:10.1175/1520-0469(2002)059<1086:Lsrr>2.0.Co;2

Boersma K F, Eskes H J, Meijer E W and Kelder H M 2005 Estimates of lightning NOx production from GOME satellite observations *Atmos Chem Phys* **5** 2311-31. doi:10.5194/acp-5-2311-2005

Bozóki T, Sátori G, Williams E, Guha A, Liu Y, Steinbach P, Leal A, Herein M, Atkinson M, Beggan C D, DiGangi E, Koloskov A, Kulak A, LaPierre J, Milling D K, Mlynarczyk J, Neska A, Potapov A, Raita T, Rawat R, Said R, Sinha A K and Yampolski Y 2023 Day-To-Day Quantification of Changes in Global Lightning Activity Based on Schumann Resonances *J Geophys Res-Atmos* **128**. doi:10.1029/2023JD038557

Brisson E, Blahak U, Lucas-Picher P, Purr C and Ahrens B 2021 Contrasting lightning projection using the lightning potential index adapted in a convection-permitting regional climate model *Clim Dynam* **57** 2037-51. doi:10.1007/s00382-021-05791-z

Brune W H, McFarland P J, Bruning E, Waugh S, MacGorman D, Miller D O, Jenkins J M, Ren X, Mao J and Peischl J 2021 Extreme oxidant amounts produced by lightning in storm clouds *Science* **372** 711-+. doi:10.1126/science.abg0492

Cecil D 2025 Reprocessed Lightning Imaging Sensor Climatology (LISCLIMO) doi:10.5067/LIS/LISCLIMO/DATA101

Cecil D J, Buechler D E and Blakeslee R J 2014 Gridded lightning climatology from TRMM-LIS and OTD: Dataset description *Atmos Res* **135** 404-14. doi:10.1016/j.atmosres.2012.06.028

Cecil D J, Buechler D E, Lang T J, Virts K S and Mach D M 2026a Lightning Climatology Datasets from TRMM LIS, ISS LIS, and OTD *J Appl Meteorol Clim* **65** 51-72. doi:10.1175/Jamc-D-25-0110.1

Cecil D J, Buechler D E, Lang T J, Virts K S and Mach D M 2026b Lightning Imaging Sensor (LIS) and Optical Transient Detector (OTD) Missions, 1995-2023 *B Am Meteorol Soc* **107** E404-E18. doi:10.1175/Bams-D-24-0268.1

Charn A B and Parishani H 2021 Predictive Proxies of Present and Future Lightning in a Superparameterized Model *J Geophys Res-Atmos* **126**. doi:10.1029/2021JD035461

Chen Y, Romps D M, Seeley J T, Veraverbeke S, Riley W J, Mekonnen Z A and Randerson J T 2021 Future increases in Arctic lightning and fire risk for permafrost carbon *Nat Clim Change* **11** 404-+. doi:10.1038/s41558-021-01011-y

Cheng W-Y 2021 Lightning Parameterization and Prediction: Conventional and Data-Driven Approaches. In: *Department of Atmospheric Sciences*: University of Washington)

Cheng W Y, Kim D and Holzworth R H 2021 CAPE Threshold for Lightning Over the Tropical Ocean *J Geophys Res-Atmos* **126**. doi:10.1029/2021JD035621

Clark S K, Ward D S and Mahowald N M 2017 Parameterization-based uncertainty in future lightning flash density *Geophys Res Lett* **44** 2893-901. doi:10.1002/2017gl073017

Cummings K A, Pickering K E, Barth M C, Bela M M, Li Y, Allen D, Bruning E, MacGorman D R, Ziegler C L, Biggerstaff M I, Fuchs B, Davis T, Carey L, Mecikalski R M and Finney D L 2024 Evaluation of Lightning Flash Rate Parameterizations in a Cloud-Resolved WRF-Chem Simulation of the 29-30 May 2012 Oklahoma Severe Supercell System Observed During DC3 *J Geophys Res-Atmos* **129**. doi:10.1029/2023JD039492

Dang R, Jacob D J, Wang H, Nowlan C R, Gonzalez Abad G, Chong H, Liu X, Shah V, Yang L H, Oak Y J, Marais E A, Horner R P, Rollins A W, Crawford J H, Li K and Liao H 2025 High-resolution geostationary satellite observations of free tropospheric NO(2) over North America and implications for lightning emissions *Proc Natl Acad Sci U S A* **122** e2510535122. doi:10.1073/pnas.2510535122

Etten-Bohm M, Yang J, Schumacher C and Jun M Y 2021 Evaluating the Relationship Between Lightning and the Large-Scale Environment and its Use for Lightning Prediction in Global Climate Models *J Geophys Res-Atmos* **126**. doi:10.1029/2020JD033990

Felsberg A, Kloster S, Wilkenskjeld S, Krause A and Lasslop G 2018 Lightning Forcing in Global Fire Models: The Importance of Temporal Resolution *J Geophys Res-Biogeo* **123** 168-77. doi:10.1002/2017jg004080

Field P R, Roberts M J and Wilkinson J M 2018 Simulated Lightning in a Convection Permitting Global Model *J Geophys Res-Atmos* **123** 9370-7. doi:10.1029/2018jd029295

Fierro A O, Mansell E R, MacGorman D R and Ziegler C L 2013 The Implementation of an Explicit Charging and Discharge Lightning Scheme within the WRF-ARW Model: Benchmark Simulations of a Continental Squall Line, a Tropical Cyclone, and a Winter Storm *Mon Weather Rev* **141** 2390-415. doi:10.1175/Mwr-D-12-00278.1

Finney D L, Doherty R M, Wild O and Abraham N L 2016a The impact of lightning on tropospheric ozone chemistry using a new global lightning parametrisation *Atmos Chem Phys* **16** 7507-22. doi:10.5194/acp-16-7507-2016

Finney D L, Doherty R M, Wild O, Huntrieser H, Pumphrey H C and Blyth A M 2014 Using cloud ice flux to parametrise large-scale lightning *Atmos Chem Phys* **14** 12665-82. doi:10.5194/acp-14-12665-2014

Finney D L, Doherty R M, Wild O, Stevenson D S, MacKenzie I A and Blyth A M 2018 A projected decrease in lightning under climate change *Nat Clim Change* **8** 210-+. doi:10.1038/s41558-018-0072-6

Finney D L, Doherty R M, Wild O, Young P J and Butler A 2016b Response of lightning NOx emissions and ozone production to climate change: Insights from the Atmospheric Chemistry and Climate Model Intercomparison Project *Geophys Res Lett* **43** 5492-500. doi:10.1002/2016gl068825

Finney D L, Marsham J H, Wilkinson J M, Field P R, Blyth A M, Jackson L S, Kendon E J, Tucker S O and Stratton R A 2020 African Lightning and its Relation to Rainfall and Climate Change in a Convection-Permitting Model *Geophys Res Lett* **47**. doi:10.1029/2020GL088163

Flemming J, Huijnen V, Arteta J, Bechtold P, Beljaars A, Blechschmidt A M, Diamantakis M, Engelen R J, Gaudel A, Inness A, Jones L, Josse B, Katragkou E, Marecal V, Peuch V H, Richter A, Schultz M G, Stein O and Tsikerdekis A 2015 Tropospheric chemistry in the Integrated Forecasting System of ECMWF *Geosci Model Dev* **8** 975-1003. doi:10.5194/gmd-8-975-2015

Gatlin P, Lang T, Quick M, Remington J, Koshak B, Cecil D, Schultz C, Bang S, Behnke S, Edens H, Bitzer P and Stough S 2023 Cubespark: A New Satellite-Based 3d Lightning Observing Concept. In: *103rd Annual Meeting of the AMS,*

Ghosh S, Cholakian A, Mailler S and Menut L 2025 Representing improved tropospheric ozone distribution over the Northern Hemisphere by including lightning NOx emissions in CHIMERE *Atmos Chem Phys* **25** 6273-97. doi:10.5194/acp-25-6273-2025

Gordillo-Vázquez F J, Pérez-Invernón F J, Huntrieser H and Smith A K 2019 Comparison of Six Lightning Parameterizations in CAM5 and the Impact on Global Atmospheric Chemistry *Earth Space Sci* **6** 2317-46. doi:10.1029/2019ea000873

Grewe V, Brunner D, Dameris M, Grenfell J L, Hein R, Shindell D and Staehelin J 2001 Origin and variability of upper tropospheric nitrogen oxides and ozone at northern mid-latitudes *Atmos Environ* **35** 3421-33. doi:10.1016/S1352-2310(01)00134-0

Guryanov V V, Mikhailov R P and Eliseev A V 2024 Present-day and future lightning frequency as simulated by four CMIP6 models *Pure Appl Geophys* **181** 3351-74. doi:10.1007/s00024-024-03587-w

He Y F, Hoque H M S and Sudo K 2022 Introducing new lightning schemes into the CHASER (MIROC) chemistry-climate model *Geosci Model Dev* **15** 5627-50. doi:10.5194/gmd-15-5627-2022

Holzworth R H, Brundell J B, McCarthy M P, Jacobson A R, Rodger C J and Anderson T S 2021 Lightning in the Arctic *Geophys Res Lett* **48**. doi:10.1029/2020GL091366

Jacobson A R and Heavner M J 2005 Comparison of narrow bipolar events with ordinary lightning as proxies for severe convection *Mon Weather Rev* **133** 1144-54. doi:10.1175/Mwr2915.1

Jenkins J M, Brune W H and Miller D O 2021 Electrical Discharges Produce Prodigious Amounts of Hydroxyl and Hydroperoxyl Radicals *J Geophys Res-Atmos* **126**. doi:10.1029/2021JD034557

Kahraman A, Kendon E J, Fowler H J and Wilkinson J M 2022 Contrasting future lightning stories across Europe *Environ Res Lett* **17**. doi:10.1088/1748-9326/ac9b78

Kaplan J O 2026 The World Wide Lightning Location Network (WWLLN) Global Lightning Climatology (WGLC) and time series doi:10.5281/zenodo.20277101

Kaplan J O and Lau K H K 2021 The WGLC global gridded lightning climatology and time series *Earth Syst Sci Data* **13** 3219-37. doi:10.5194/essd-13-3219-2021

Kaplan J O and Lau K H K 2022 World Wide Lightning Location Network (WWLLN) Global Lightning Climatology (WGLC) and time series, 2022 update *Earth Syst Sci Data* **14** 5665-70. doi:10.5194/essd-14-5665-2022

Kawazoe S, Sato Y and Hayashi S 2025 Investigating the Uncertainties in Future Lightning Activity over Eastern Japan Using Convective-Permitting Climate Simulations *Sola* **21b** 18-27. doi:10.2151/sola.21B-003

Krause A, Gregor K, Meyer B F and Rammig A 2025 Simulating Lightning-Induced Tree Mortality in the Dynamic Global Vegetation Model LPJ-GUESS *Global Change Biol* **31**. doi:10.1111/gcb.70312

Krause A, Gregor K, Qu Y, Veraverbeke S and Rammig A accepted Large Projected Increase in Cloud-to-Ground Lightning Under Future Climate *Earth's Future*.

Krause A, Kloster S, Wilkenskjeld S and Paeth H 2014 The sensitivity of global wildfires to simulated past, present, and future lightning frequency *J Geophys Res-Biogeo* **119** 312-22. doi:10.1002/2013jg002502

Krause A and Rammig A submitted A Simple Climatology Benchmark Outperforms Machine-Learning Lightning Parameterizations. doi:10.22541/essoar.15010630/v1

Lamarque J F, Kiehl J T, Brasseur G P, Butler T, Cameron-Smith P, Collins W D, Collins W J, Granier C, Hauglustaine D, Hess P G, Holland E A, Horowitz L, Lawrence M G, McKenna D, Merilees P, Prather M J, Rasch P J, Rotman D, Shindell D and Thornton P 2005 Assessing future nitrogen deposition and carbon cycle feedback using a multimodel approach: Analysis of nitrogen deposition *J Geophys Res-Atmos* **110**. doi:10.1029/2005jd005825

Lavigne T, Liu C T and Liu N N 2019 How Does the Trend in Thunder Days Relate to the Variation of Lightning Flash Density? *J Geophys Res-Atmos* **124** 4955-74. doi:10.1029/2018jd029920

Liaskos C E, Allen D J and Pickering K E 2015 Sensitivity of tropical tropospheric composition to lightning NOx production as determined by replay simulations with GEOS-5 *J Geophys Res-Atmos* **120** 8512-34. doi:10.1002/2014jd022987

Lopez P 2016 A Lightning Parameterization for the ECMWF Integrated Forecasting System *Mon Weather Rev* **144** 3057-75. doi:10.1175/Mwr-D-16-0026.1

Luhar A K, Galbally I E, Woodhouse M T and Abraham N L 2021 Assessing and improving cloud-height-based parameterisations of global lightning flash rate, and their impact on lightning-produced NOx and tropospheric composition in a chemistry-climate model *Atmos Chem Phys* **21** 7053-82. doi:10.5194/acp-21-7053-2021

Ma M, Tao S C, Zhu B Y, Lü W T and Tan Y B 2005 Response of global lightning activity to air temperature variation *Chinese Sci Bull* **50** 2640-4. doi:10.1360/04wd0351

Mackerras D, Darveniza M, Orville R E, Williams E R and Goodman S J 1998 Global lightning: Total, cloud and ground flash estimates *J Geophys Res-Atmos* **103** 19791-809. doi:10.1029/98jd01461

Magi B I 2015 Global Lightning Parameterization from CMIP5 Climate Model Output *J Atmos Ocean Tech* **32** 434-52. doi:10.1175/Jtech-D-13-00261.1

Mao J Q, Zhao T L, Keller C A, Wang X, McFarland P J, Jenkins J M and Brune W H 2021 Global Impact of Lightning-Produced Oxidants *Geophys Res Lett* **48**. doi:10.1029/2021GL095740

McCaul E W, Goodman S J, LaCasse K M and Cecil D J 2009 Forecasting Lightning Threat Using Cloud-Resolving Model Simulations *Weather Forecast* **24** 709-29. doi:10.1175/2008waf2222152.1

Meijer E W, van Velthoven P F J, Brunner D W, Huntrieser H and Kelder H 2001 Improvement and evaluation of the parameterisation of nitrogen oxide production by lightning *Phys Chem Earth Pt C* **26** 577-83. doi:10.1016/S1464-1917(01)00050-2

Michalon N, Nassif A, Saouri T, Royer J F and Pontikis C A 1999 Contribution to the climatological study of lightning *Geophys Res Lett* **26** 3097-100. doi:10.1029/1999gl010837

Michibata T 2024 Significant increase in graupel and lightning occurrence in a warmer climate simulated by prognostic graupel parameterization *Sci Rep-Uk* **14**. doi:10.1038/s41598-024-54544-5

Murphy M J and Said R K 2020 Comparisons of Lightning Rates and Properties From the US National Lightning Detection Network (NLDN) and GLD360 With GOES-16 Geostationary Lightning Mapper and Advanced Baseline Imager Data *J Geophys Res-Atmos* **125**. doi:10.1029/2019JD031172

Murray L T 2018 An uncertain future for lightning *Nat Clim Change* **8** 191-2. doi:10.1038/s41558-018-0094-0

Murray L T, Jacob D J, Logan J A, Hudman R C and Koshak W J 2012 Optimized regional and interannual variability of lightning in a global chemical transport model constrained by LIS/OTD satellite data *J Geophys Res-Atmos* **117**. doi:10.1029/2012jd017934

Nag A, Murphy M J, Schulz W and Cummins K L 2015 Lightning locating systems: Insights on characteristics and validation techniques *Earth Space Sci* **2** 65-93. doi:10.1002/2014ea000051

Ni X, Hui W, Zhang Q H, Huang F X and Liu C T 2021 Comparison of Lightning Detection Between the FY-4A Lightning Mapping Imager and the ISS Lightning Imaging Sensor *Earth Space Sci* **8**. doi:ARTN e2020EA001099 10.1029/2020EA001099

Pasko V P, Celestin S, Bourdon A, Janalizadeh R, Pervez Z, Jansky J and Gourbin P 2025 Photoelectric Effect in Air Explains Lightning Initiation and Terrestrial Gamma Ray Flashes *J Geophys Res-Atmos* **130**. doi:10.1029/2025JD043897

Pérez-Invernón F J, Gordillo-Vázquez F J, Huntrieser H and Jöckel P 2023 Variation of lightning-ignited wildfire patterns under climate change *Nat Commun* **14**. doi:10.1038/s41467-023-36500-5

Pérez-Invernón F J, Gordillo-Vázquez F J, Huntrieser H, Jöckel P and Bucsela E J 2025 Sensitivity of climate-chemistry model simulated atmospheric composition to the application of an inverse relationship between NOx emission and lightning flash frequency *Atmos Chem Phys* **25** 5557-75. doi:10.5194/acp-25-5557-2025

Pérez-Invernón F J, Gordillo-Vázquez F J, Smith A K, Arnone E and Winkler H 2019 Global Occurrence and Chemical Impact of Stratospheric Blue Jets Modeled With WACCM4 *J Geophys Res-Atmos* **124** 2841-64. doi:10.1029/2018jd029593

Pickering K E, Allen D J and Huntrieser H 2026 The Role of Lightning in Atmospheric Chemistry *J Geophys Res-Atmos* **131**. doi:10.1029/2026JD046484

Prentice S A and Mackerras D 1977 The Ratio of Cloud to Cloud-Ground Lightning Flashes in Thunderstorms *J Appl Meteorol Clim* **16**. doi:10.1175/1520-0450(1977)016<0545:TROCTC>2.0.CO;2

Price C 2016 ELF Electromagnetic Waves from Lightning: The Schumann Resonances *Atmosphere-Basel* **7**. doi:10.3390/atmos7090116

Price C, Penner J and Prather M 1997 NOx from lightning .1. Global distribution based on lightning physics *J Geophys Res-Atmos* **102** 5929-41. doi:10.1029/96jd03504

Price C and Rind D 1992 A Simple Lightning Parameterization for Calculating Global Lightning Distributions *J Geophys Res-Atmos* **97** 9919-33. doi:10.1029/92jd00719

Price C and Rind D 1993 What Determines the Cloud-to-Ground Lightning Fraction in Thunderstorms *Geophys Res Lett* **20** 463-6. doi:10.1029/93gl00226

Price C and Rind D 1994a The Impact of a 2-X-Co2 Climate on Lightning-Caused Fires *J Climate* **7** 1484-94. doi:10.1175/1520-0442(1994)007<1484:Tioacc>2.0.Co;2

Price C and Rind D 1994b Modeling Global Lightning Distributions in a General-Circulation Model *Mon Weather Rev* **122** 1930-9. doi:10.1175/1520-0493(1994)122<1930:Mgldia>2.0.Co;2

Price C and Rind D 1994c Possible Implications of Global Climate-Change on Global Lightning Distributions and Frequencies *J Geophys Res-Atmos* **99** 10823-31. doi:10.1029/94jd00019

Price C G 2013 Lightning Applications in Weather and Climate Research *Surv Geophys* **34** 755-67. doi:10.1007/s10712-012-9218-7

Qie X S, Yair Y, Di S X, Huang Z F and Jiang R B 2024 Lightning response to temperature and aerosols *Environ Res Lett* **19**. doi:10.1088/1748-9326/ad63bf

Qu Y, Brambleby E, Janssen T, Moris J, Said R, Murphy M, Hunt H, Joshi M, Mataveli G, Pérez Invernón F J, Yebra M, Zhao L, Jones M and Veraverbeke S 2026 FLASHMAP: A Global Gridded Cloud-to-Ground and Intra-Cloud Lightning Dataset [Dataset] doi:https://doi.org/10.5281/zenodo.18925362

Reeve N and Toumi R 1999 Lightning activity as an indicator of climate change *Q J Roy Meteor Soc* **125** 893-903. doi:10.1002/qj.49712555507

Ringhausen J, Bitzer P, Koshak W and Mecikalski J 2021 Classification of GLM Flashes Using Random Forests *Earth Space Sci* **8**. doi:10.1029/2021EA001861

Romps D M 2019 Evaluating the Future of Lightning in Cloud-Resolving Models *Geophys Res Lett* **46** 14863-71. doi:10.1029/2019gl085748

Romps D M, Charn A B, Holzworth R H, Lawrence W E, Molinari J and Vollaro D 2018 CAPE Times P Explains Lightning Over Land But Not the Land-Ocean Contrast *Geophys Res Lett* **45** 12623-30. doi:10.1029/2018gl080267

Romps D M, Seeley J T, Vollaro D and Molinari J 2014 Projected increase in lightning strikes in the United States due to global warming *Science* **346** 851-4. doi:10.1126/science.1259100

Rudlosky S D, Goodman S J, Virts K S and Bruning E C 2019 Initial Geostationary Lightning Mapper Observations *Geophys Res Lett* **46** 1097-104. doi:10.1029/2018gl081052

Santer B D, Sausen R, Wigley T M L, Boyle J S, AchutaRao K, Doutriaux C, Hansen J E, Meehl G A, Roeckner E, Ruedy R, Schmidt G and Taylor K E 2003 Behavior of tropopause height and atmospheric temperature in models, reanalyses, and observations: Decadal changes - art. no. 4002 *J Geophys Res-Atmos* **108**. doi:10.1029/2002jd002258

Saunders C P R 1993 A Review of Thunderstorm Electrification Processes *J Appl Meteorol* **32** 642-55. doi:10.1175/1520-0450(1993)032<0642:Arotep>2.0.Co;2

Schumann U and Huntrieser H 2007 The global lightning-induced nitrogen oxides source *Atmos Chem Phys* **7** 3823-907. doi:10.5194/acp-7-3823-2007

Soler S, Gordillo-Vázquez F J, Pérez-Invernón F J, Jöckel P, Neubert T, Chanrion O, Reglero V and Ostgaard N 2024 Parameterizations for global thundercloud corona discharge distributions *Atmos Chem Phys* **24** 10225-43. doi:10.5194/acp-24-10225-2024

Soler S, Pérez-Invernón F J, Gordillo-Vázquez F J, Luque A, Li D, Malagón-Romero A, Neubert T, Chanrion O, Reglero, Navarro-Gonzalez J, Lu G, Zhang H, Huang A and Ostgaard N 2020 Blue Optical Observations of Narrow Bipolar Events by ASIM Suggest Corona Streamer Activity in Thunderstorms *J Geophys Res-Atmos* **125**. doi:10.1029/2020JD032708

Stolz D C, Bilsback K R, Pierce J R and Rutledge S A 2021 Evaluating Empirical Lightning Parameterizations in Global Atmospheric Models *J Geophys Res-Atmos* **126**. doi:10.1029/2020JD033695

Stolz D C, Rutledge S A, Pierce J R and van den Heever S C 2017 A global lightning parameterization based on statistical relationships among environmental factors, aerosols, and convective clouds in the TRMM climatology *J Geophys Res-Atmos* **122** 7461-92. doi:10.1002/2016jd026220

Takahashi T 1978 Riming Electrification as a Charge Generation Mechanism in Thunderstorms *J Atmos Sci* **35** 1536-48. doi:10.1175/1520-0469(1978)035<1536:Reaacg>2.0.Co;2

Thornhill G, Collins W, Olivi D, Skeie R B, Archibald A, Bauer S, Checa-Garcia R, Fiedler S, Folberth G, Gjermundsen A, Horowitz L, Lamarque J F, Michou M, Mulcahy J, Nabat P, Naik V, O'Connor F M, Paulot F, Schulz M, Scott C E, Séférian R, Smith C, Takemura T, Tilmes S, Tsigaridis K and Weber J 2021 Climate-driven chemistry and aerosol feedbacks in CMIP6 Earth system models *Atmos Chem Phys* **21** 1105-26. doi:10.5194/acp-21-1105-2021

Tost H, Jöckel P J and Lelieveld J 2007 Lightning and convection parameterisations -: uncertainties in global modelling *Atmos Chem Phys* **7** 4553-68. doi:10.5194/acp-7-4553-2007

Uribe A, Contizanetti M, Bender F A M and Mauritsen T 2026 Icon simulations suggest model-dependent cloud feedbacks in global storm-resolving models *Clim Dynam* **64**. doi:10.1007/s00382-026-08235-8

Verjans V and Franzke C L E 2025 Development of a Data-Driven Lightning Scheme for Implementation in Global Climate Models *J Adv Model Earth Sy* **17**. doi:10.1029/2024MS004464

Verjans V, Franzke C L E, Lee S S, Kim I W, Tilmes S, Lawrence D M, Vitt F and Li F 2025 Quantifying CO2 forcing effects on lightning, wildfires, and climate interactions *Sci Adv* **11**. doi:10.1126/sciadv.adt5088

Vonnegut B 1963 Some facts and speculation concerning the origin and role of thunderstorm electricity *Meteorol. Monogr.* **5** 24-241.

Wang X B, Zhang Y Z, Bozóki T, Liang R S, Xie X C, Zhao S T, Wang R, Zhao Y J and Sun S 2025 Contributions of lightning to long-term trends and inter-annual variability in global atmospheric chemistry constrained by Schumann resonance observations *Atmos Chem Phys* **25** 8929-42. doi:10.5194/acp-25-8929-2025

Whaley C, Etten-Bohm M, Schumacher C, Akingunola A, Arora V, Cole J, Lazare M, Plummer D, von Salzen K and Winter B 2024 A new lightning scheme in the Canadian Atmospheric Model (CanAM5.1): implementation, evaluation, and projections of lightning and fire in future climates *Geosci Model Dev* **17** 7141-55. doi:10.5194/gmd-17-7141-2024

Williams E and Stanfill S 2002 The physical origin of the land-ocean contrast in lightning activity *Cr Phys* **3** 1277-92. doi:10.1016/S1631-0705(02)01407-X

Williams E R 1985 Large-Scale Charge Separation in Thunderclouds *J Geophys Res-Atmos* **90** 6013-25. doi:10.1029/JD090iD04p06013

Williams E R 1992 The Schumann Resonance - a Global Tropical Thermometer *Science* **256** 1184-7. doi:10.1126/science.256.5060.1184

Williams E R 1994 Global Circuit Response to Seasonal-Variations in Global Surface Air-Temperature *Mon Weather Rev* **122** 1917-29. doi:10.1175/1520-0493(1994)122<1917:Gcrtsv>2.0.Co;2

Williams E R 2005 Lightning and climate: A review *Atmos Res* **76** 272-87. doi:10.1016/j.atmosres.2004.11.014

Wong J, Barth M C and Noone D 2013 Evaluating a lightning parameterization based on cloud-top height for mesoscale numerical model simulations *Geosci Model Dev* **6** 429-43. doi:10.5194/gmd-6-429-2013

Wu Y, Pour-Biazar A, Koshak W J and Cheng P 2023 LNOx Emission Model for Air Quality and Climate Studies Using Satellite Lightning Mapper Observations *J Geophys Res-Atmos* **128**. doi:10.1029/2022JD037406

Yair Y 2018 Lightning hazards to human societies in a changing climate *Environ Res Lett* **13**. doi:10.1088/1748-9326/aaea86

Yair Y, Lynn B, Price C, Kotroni V, Lagouvardos K, Morin E, Mugnai A and Llasat M D 2010 Predicting the potential for lightning activity in Mediterranean storms based on the Weather Research and Forecasting (WRF) model dynamic and microphysical fields *J Geophys Res-Atmos* **115**. doi:10.1029/2008jd010868

Yanoviak S P, Gora E M, Bitzer P M, Burchfield J C, Muller-Landau H C, Detto M, Paton S and Hubbell S P 2020 Lightning is a major cause of large tree mortality in a lowland neotropical forest *New Phytol* **225** 1936-44. doi:10.1111/nph.16260

Yin M, Wang Y, Fang Y, Li F, Qie X S, Wang Y Y, Wei D M, Yuan H H, Ji Y P, Zhang Y and Liu J 2026 A Two-Dimensional Deep Learning Scheme With One Predicator Only to Parametrize Global Lightning *Geophys Res Lett* **53**. doi:10.1029/2025GL120502

Yoshida S, Morimoto T, Ushio T and Kawasaki Z 2009 A fifth-power relationship for lightning activity from Tropical Rainfall Measuring Mission satellite observations *J Geophys Res-Atmos* **114**. doi:10.1029/2008jd010370

Zhu Y A, Stock M, Lapierre J and DiGangi E 2022 Upgrades of the Earth Networks Total Lightning Network in 2021 *Remote Sens-Basel* **14**. doi:10.3390/rs14092209